Molecular dynamics simulations of the effect of solvent on PSS/PDADMA polyelectrolyte interactions

Anna Leino

School of Chemical Engineering

Thesis submitted for examination for the degree of Master of Science in Technology.

Espoo 26.9.2018

Supervisor

Prof. Sami Franssila

Advisor

Dr. Maria Sammalkorpi

Aalto University
School of Chemical Engineering

Aalto University
School of Chemical
Engineering

Aalto University, P.O. BOX 11000, 00076 AALTO
www.aalto.fi
Abstract of the master's thesis

Author Anna Leino

Title Molecular dynamics simulations of the effect of solvent on PSS/PDADMA polyelectrolyte interactions

Degree programme Chemical, Biochemical and Materials Engineering

Major Functional Materials **Code of major** CHEM3025

Supervisor Prof. Sami Franssila

Advisor Dr. Maria Sammalkorpi

Date 26.9.2018 **Number of pages** 9+68 **Language** English

Abstract

Oppositely charged polymers, polyelectrolytes, assemble spontaneously in aqeous solutions forming materials with a broad range of interesting and tunable properties, such as superhydrophobicity. Solvent composition is known to affect the properties of polyelectrolyte assemblies. Water plasticizes these materials, whereas addition of certain organic solvents results in dehydration of the assembly. Solvent also affects thermal softening of polyelectrolyte materials. Although these effects are well-known macroscopicly, the reasons and phenomena behind the solvent effects are not fully resolved. These phenomena are difficult to study by experimental means. Thus, to extend the current knowledge on solvent effects on polyelectrolyte complexes, this study presents molecular dynamics simulations on the effect of ethanol and urea on the interactions of polyelectrolyte complex formed by one PSS chain and one PDADMA chain. 10 wt% and 30 wt% ethanol and urea solutions are compared to pure water. The results reveal changes in polyelectrolyte complex hydration shell structure, solvent dynamics and counterion condensation. Urea increases the PSS-PDADMA separation, which implies that it could soften polyelectrolyte assemblies. The results indicate that ethanol could change salt effects on polyelectrolyte complexes. Both ethanol and urea slow down solvent diffusion, which could result in increased solvent stability. This study provides new insights to the effects of solvent structure and dynamics on polyelectrolyte complexes and suggests that both ethanol and urea could be utilized to tune the properties of polyelectrolyte assemblies.

Keywords molecular dynamics, polyelectrolytes, PDADMA, PSS, PEC , PEM, polyelectrolyte multilayer, polyelectrolyte complex

Aalto University
School of Chemical
Engineering

Aalto-yliopisto, PL 11000, 00076 AALTO
www.aalto.fi
Diplomityön tiivistelmä

Tekijä Anna Leino

Työn nimi Molekyylidynaamiset simulaatiot liuottimen vaikutuksesta PSS- ja PDADMA-polyelektrolyyttien vuorovaikutuksiin

Koulutusohjelma Chemical, Biochemical and Materials Engineering

Pääaine Functional Materials **Pääaineen koodi** CHEM3025

Työn valvoja Prof. Sami Franssila

Työn ohjaaja TkT Maria Sammalkorpi

Päivämäärä 26.9.2018 **Sivumäärä** 9+68 **Kieli** Englanti

Tiivistelmä

Vastakkaisvaraukselliset polymeerit, polyelektrolyytit, muodostavat vesiliuoksessa spontaanisti materiaaleja, joilla on paljon mielenkiintoisia ja muokattavia ominaisuuksia, mm. superhydrofobisuus. Liuottimen koostumuksen tiedetään vaikuttavan polyelektrolyyttimateriaalien ominaisuuksiin. Vesi pehmentää näitä materiaaleja, kun taas tietyt orgaaniset liuottimet poistavat vettä polyelektrolyyttikomplekseista. Liuotin vaikuttaa myös lämpötilan muutoksen aiheuttamiin faasitransitioihin. Vaikka liuottimen vaikutukset tunnetaan hyvin makroskooppisten ominaisuuksien tasolla, ilmiöiden mikroskooppiset syyt ovat vielä selvittämättä. Kyseisten ilmöiden havainnoiminen on vaikeaa kokeellisin menetelmin. Tämä diplomityö tutkii molekyylidynaamisten simulaatioiden avulla etanolin ja urean vaikutusta yhdestä PSS-ketjusta ja yhdestä PDADMA-ketjusta koostuvan polyelektrolyyttikompleksin vuorovaikutuksille. 10 wt%:n ja 30 wt%:n urea- ja etanoliluoksia vertaillaan vesiliuokseen. Tulokset osoittavat, että urea ja etanoli muuttavat polyelektrolyyttikompleksia ympäröivän hydraatiokerroksen rakennetta, sekä liuottimen dynamiikkaa ja vastaionikondensaatiota. Urea loitontaa polyelektrolyyttiketjuja toisistaan. Tulokset siis implikoivat, että urea voisi mahdollisesti pehmentää polyelektrolyyttimateriaaleja. Tulokset osoittavat myös, että etanoli saattaisi muuttaa suolan vaikutusta polyelektrolyyttikompleksiin. Tämä diplomityö avaa uusia näkökulmia liuottimen rooliin polyelektrolyyttikomplekseissa, ja esittää, että sekä etanolia että ureaa voisi hyödyntää polyelektrolyyttimateriaalien ominaisuuksien säätelemiseen.

Avainsanat molekyylidynamiikka, polyelektrolyytit, PDADMA, PSS, PEC, PEM, polyelektrolyyttikompleksi

Preface

This thesis work was conducted in the spring and summer of 2018 in the research group of Soft Materials Modelling at the School of Chemical Engineering at Aalto University.

Firstly, I want to thank my supervisor professor Sami Franssila, my advisor Maria Sammalkorpi and Dr. Piotr Batys for providing me with an inspiring topic and guiding me through this project. I am grateful for the many fruitful conversations an delightful moments I have had with my fellow office mates, who have also provided irreplacable peer support throughout the thesis process.

Lastly, I want to thank my boyfriend, friends and family for their endless support, encouragement and understanding troughout this whole process.

Otaniemi, 26.9.2018

Anna Leino

Contents

Symbols and abbreviations

Symbols

l_B	Bjerrum length
e	elementary charge
ε	dielectric constant of the medium
k_B	Boltzmann's constant
T	absolute temperature
ξ	Debye length
n	particle density for Debye length
q_0	Manning parameter
l	charge/length for Manning parameter
ϕ	electrostatic potential
ρ	density
$n_{0,i}$	number density of the i^{th} ion species at zero electrostatic potential
q	charge of a particle
R_g	Radius of gyration
N	number of monomers in polymer chain
$\mathbf{r}_{cm}$	position vector of centre of mass
$\mathbf{r}_i$	position vector of i^{th} monomer of a polymer chain
ϕ^*	polymer overlap volume fraction
c^*	polymer overlap concentration
V_{mon}	monomer volume
N_A	Avogadro's number
V	solution volume
b	monomer diameter
R	size of a polymer chain coil
E_{tot}	total energy
E_{bonds}	bond stretching energy in empirical force-field
E_{angles}	angle bending energy in empirical force-field
$E_{dihedrals}$	dihedral angles energy in empirical force-field
$E_{non-bonded}$	non-bonded interactions energy in empirical force-field
K_r	spring constant for bonds in empirical force-field
r_{eq}	equilibrium length of a bond in empirical force-field
K_θ	spring constant for angle between bonds in empirical force-field
θ_{eq}	equilibrium angle in empirical force-field
V_1, V_2, V_3	torsional terms in empirical force-field
ϕ	measured dihedral angle
q_i, q_j	charges of particles i and j
r	distance between two particles
ϵ	potential well depth
F	force
m	mass
a	acceleration

Δt	time step
$\mathbf{b}$	third derivative of particle position
t	time
$F_n(t)$	force on a particle n
$r_n(t)$	position of particle n at time t
$\langle \rho_B \rangle$	the density of particles B at a distance r from particle A for radial distribution fu
$C(\tau)$	autocorrelation of two measurements as a fucntion of time delay τ
$s_i(t)$	signal (time dependent, for autocorrelation calculation)
τ	time delay between two measurement values
D_A	diffusion coefficient for particle group A
$r_i(t)$	molecule position at time t
D_w	diffusion coefficient of water
$D_{Additive}$	diffusion coefficient of additive (ethanol/urea)

Abbreviations

PE	polyelectrolyte
PEC	polyelectrolyte complex
PEM	polyelectrolyte multilayer
MD	molecular dynamics
PSS	polystyrene sulfonate
PDADMA	polydiallyldimethylammonium
PB	Poisson-Boltzmann equation
LbL	layer-by-layer assembly
MDSC	modulated differential scanning calorimetry
MC	Monte Carlo modelling
OPLS-aa	Optimised Potentials for Liquid Simulations All Atom Force Field
PBC	periodic boundary conditions
RDF	radial distribution function
SD	standard deviation

1 Introduction

Polyelectrolytes (PEs) are charged macromolecules. Like other polymers, they are chains built from repeating structure units, monomers. However, unlike many other polymers, they dissolve in aqueous solutions by dissociating into a charged macromolecule and its counterions. Oppositely charged PEs can associate forming assemblies with different morphologies, resulting in a variety of soft materials with a wide range of properties, such as superhydrophobicity, super tensility or responsiveness to changes in the sourrounding environment[1]. Due to the mentioned unusual properties and their potential in industry and applications, PEs and self-assembled PE structures have been extensively studied, and the interest towards these materials has grown during the last decades[1–3].

Polyelectrolyte materials include a large amount of important and interesting materials. For instance, many molecules of biological importance, such as DNA and polypeptides are PEs. Spontaneously forming polyelectrolyte assemblies, polyelectrolyte complexes (PECs) and polyelectrolyte multilayers (PEMs) have many possible applications. PEMs are PE structures that consists of alternating layers of polyanions and polycations[3]. They are produced using so-called layer-by-layer methods, where the PE membrane is constructed by depositing alternately negatively and positively charged polymers on a substrate of choice[3].

A variety of easily controllable factors, such as pH[4], and the choice and amount of solvent[5] and salt[6 7 8], influence the properties of PE assemblies. Thus, by controlling these factors, the properties of the PE material can be fine-tuned to correspond to the requirements of the application. For instance, the pH-induced swelling of certain PEMs be used to obtain functional coatings, such as coatings with anti-reflective properties[9]. The formation of PEC coacervate, a fluid-fluid phase separation occurring due to electrostatics, and the resulted change in properties such as interfacial energy and friction, has been studied for use in coatings for cell-adhesion promotion in implants[10,11]. The strong influence of the chemical environment on the properties of PE materials could be developed even further: PE assemblies have demonstrated potential as stimuli-responsive materials, utilizing e.g. the change in stiffness as a function of water content[1], pH-triggered swelling[12] or temperature-triggered softening[13].

Solvent significantly affects the properties and formation of PE assemblies[14]. Both the amount and quality of the solvent have an effect on the properties of PE assemblies[14,15]. The most important solvent effect on PE assemblies is the plasticizing effect of water[15]. Dry assemblies are rigid and brittle, whereas wet PECs are elastic and soft[15]. In general, interactions between PEs result from the charges of these molecules. Polarity of solvent greatly affects the magnitude of these interactions, and the effect of solvent on PE materials is significant. When organic solvent is added to the solution, PE assemblies dehydrate, which typically results in increasing stiffness and in case of PEMs, contraction of the multilayer structure[16]. The interactions between water and organic solvents consist of hydrophobic interactions and hydrogen bonding[17]. The equilibrium of these interactions affects the uniformity of the solvent and, consequently, changes the mechanical properties of the PE assembly[16,17]. Although these described solvent effects are well known experimentally

and understood as continuum level phenomena, the microstructural origins and interactions causing these effects are yet to discover.

To extend the PE research beyond the limits of experimental techniques, molecular modelling methods, such as molecular dynamics (MD) can be employed. Modelling allows the use of isolation of the origins of the observed responses. This thesis aims to contribute to resolving the molecular level characteristics of aqueous PE systems by investigating via molecular dynamics how interactions change in polystyrene sulfonate-polydiallyldimethylammonium solution when water, which is the most common PE solvent, is replaced with water-alcohol or water-urea mixture. Polystyrene sulfonate (PSS) and polydiallyldimethylammonium (PDADMA) were chosen as the polyanion and polycation, respectively, because their experimental behaviour is well known. PSS-PDADMA-systems have been used as a model system for research on PE solutions and assemblies. The solvent additives, ethanol and urea, were chosen because they change the properties of the solvent. Ethanol decreases solvent polarity, and urea forms hydrogen-bonding networks, disturbing water hydrogen bonds[18]. They are very widely used, cheap chemicals in industry. The chemical structures of the studied PEs and solvent additives are presented in Fig. 1.

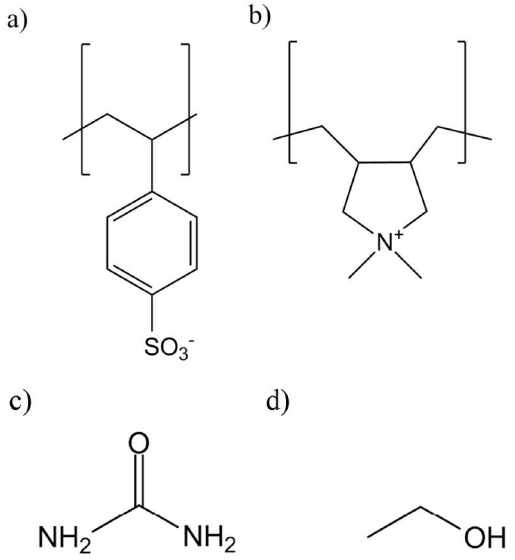

Figure 1: The chemical structures of the studied polymers and solvent additives: a) polystyrene sulfonate (PSS), b) polydiallyldimethylammonium (PDADMA), c) urea and d) ethanol.

The literature review part of this thesis introduces concepts, terminology and some basic theories crucial to the work and provides an overview of existing experimental and computational research on polyelectrolyte solutions and assemblies. The research part of the thesis consists of setting up, running, analysis and data presentation of MD (molecular dynamics) simulations of PSS-PDADMA systems at different concentrations of ethanol and urea. Chapter 3 presents the employed modelling methods, concentrating on molecular dynamics and reviewing modelling of polymeric

systems in general. Chapter 4 presents the simulation systems and techniques employed in this study. Next chapter consists of presentation and discussion of the obtained results. Chapter 6 finishes the thesis with conclusions and future perspectives of the topic.

2 Polyelectrolytes in aqueous solutions

The focus of this thesis being polyelectrolytes in solutions, this chapter presents general background on polyelectrolyte solutions and research. First, the behaviour of single polyelectrolyte chain in water is discussed. A description of systems with multiple polyelectrolytes and the association of oppositely charged chains follows.

2.1 One polyelectrolyte chain in solution

2.1.1 Polyelectrolyte dissociation in water

As described previously, PEs are charged macromolecules that have characteristics typical to polymers and electrolytes due to their ability to dissolve by dissociating to a charged macromolecule and small counterions. When a PE chain is not in aqueous solution, it is a solid, electrically neutral molecule. In aqueous solution the PE dissociates to a charged macromolecule and small counterions, forming an electrically conductive solution. Negatively charged PE is polyanion, positively charged polycation. PSS is a polyanion, PDADMA a polycation.

PEs can be classified to strong and weak by their dissociation properties. Strong PEs usually dissociate completely in solution, i.e. all of their electrolyte groups dissolve releasing a small counterion[2]. The dissociation of weak PEs, however, is dependent of the pH of the solution, and they are in most conditions partially dissociated, in other words, their charge depends on the pH, and in most conditions they are not fully charged.[2]. PSS and PDADMA, the materials studied in this thesis, are both strong PEs. PSS binds as counterions positive ions, such as sodium ions, and PDADMA negative, e.g. chloride ions.

2.1.2 Length scales of electrostatic interactions in polyelectrolyte solutions

Although many of the properties of PE solutions, such as relatively high viscosity, are also common to all polymeric solutions, there are important differences as well. For instance, the chain conformations of PEs are very different from those of uncharged polymers. These differences arise from the fact that PEs in solutions are charged. To be able to discuss the properties related to the electrostatic interactions in these solutions, it is useful to define two length scales related to the Coulombic forces in charge containing solutions. Two widely employed terms are the Bjerrum length and the Debye length. Bjerrum length

$$l_B = e^2/\varepsilon k_B T \tag{1}$$

where e is the elementary charge, ε the dielectric constant of the medium, k_B the Boltzmann's constant and T the absolute temperature, describes the length at which the Coulombic interaction of two unit charges is $k_B T$. It is useful for assessing electrostatic screening and determining when interactions of two charges are thermodynamically relevant. Bjerrum length can be used to obtain the Debye length

$$\xi = (8\pi l_B n)^{-1/2} \quad (2)$$

where n is the particle density. It determines how far the electrostatic effect of a charged species extends in solution.

2.1.3 Counterion condensation

In a typical PE solution there are three chemical species groups: the PE, the solvent and counterions. Together all of these particles and their interactions determine the properties of PE complexes and macroscopic materials. To understand the origins of the properties, the characteristics of all the particles present must be considered and understood. Although this thesis concentrates on the role of solvent on PE interactions, the role of counterions is important, as solvent quality affects the counterion condensation, and counterion-solvent interactions affect the PE-solvent interactions. Also, counterion condensation theories demonstrate the complex nature of PE solutions, and the progress made during the last decades. In this thesis, the magnitude of the counterion condensation is of interest, because it is affected by solvent quality. Condensation of counterions changes the effective charge of the PE, and as a consequence, its interactions with other PEs.

This chapter discusses and compares some most common counterion condensation theories. The counterions can be classified to two categories: free counterions and condensed counterions. The ions that are free can move in the solution volume V, whereas condensed counterions are those that remain in the vicinity of the PE chain[19]. Counterion condensation occurs when counterions associate strongly on the PEs in solution, due to electrostatic attraction between the PE and the ion. In very dilute solutions this is not favourable[19]. With increasing PE concentration the counterion condensation increases, and the fraction of free ions decreases[2,19]. Counterions affect PE interactions by changing the flexibility and effective charge of the chains, which makes counterion condensation an important phenomenon when studying PEs in solutions.

Both theoretical and modelling efforts have been made to understand the counterion condensation phenomenon. Mean-field theories such as the Poisson-Boltzmann equation have been used to estimate the charge distribution around the PE. Manning's counterion condensation[20] is another mean-field approach used to estimate counterion condensation in certain solvent at certain temperature. To extend the research outside the mean-field approaches, to explicit counterions, numerical modelling methods such as molecular mechanical approaches can be employed. Theoretical approaches beyond mean-field theories include density functional approach[21] and integral equation corrections[22].

However, despite the large number of approaches, as the exact mechanism of counterion condensation and affecting factors are very complex, the prediction of counterion condensation behaviour is extremely difficult. Additional research is especially needed for the condensation in systems that contain several different PEs[23]. The need for additional research rises from the complex nature of these systems and the wide possibilities in the applicability of PE assemblies.

The remainder of this section provides an review of the basic counterion condensation models. As this thesis study is not focused on the counterion condensation, only basic overview to the topic is provided.

Manning theory is a widely used simple model of the counterion condensation. In this theory the PE is presented as a charged cylinder. The Manning theory[20] states that a certain portion of the small counterions is always condensed on the PE, if the charge density of the polymer is above a critical limit.[24] This limit for counterion condensation to occur is described by the Manning parameter

$$q_0 = l_B/l \tag{3}$$

where l_B is Bjerrum length and l the charge/length. Counterion condensation occurs when $q_0 > 1$. The limit was predicted by Manning[20] and Oosawa[25].

Another commonly used estimation method for the counterion condensation is the Poisson-Boltzmann (PB) equation (Eq. 6). It can be used to estimate the electrostatic potential and distribution of ions in the vicinity of a macromolecule surface, often described as a uniformly charged cylinder. The Poisson-Boltzmann equation consists of Poisson's equation which gives the three-dimensional potential distribution as a function of charge density, and Boltzmann's distribution, from which local ion density is obtained. Poisson's equation

$$\varepsilon \bigtriangledown^2 \phi = -e\rho \tag{4}$$

incorporates electrostatic potential ϕ, charge density ρ, elementary charge e and dielectric permittivity of the solvent ε . This equation is commonly combined with an ion distribution that follows Boltzmann distribution

$$n_i = e^{\frac{-q_i\phi}{k_B T}} \tag{5}$$

where q is the charge of an ion of species i, e the elementary charge, ϵ the dielectric permittivity of the solvent, T the absolute temperature, k_B Boltzmann constant and $n_{0,i}$ the number density of the i^{th} ion species at zero electrostatic potential. This gives the electrostatic potential distribution around the macromolecule.

Combining Eq. 4 and 5 gives the Poisson-Boltzmann equation

$$\bigtriangledown^2 \phi = -\frac{1}{\epsilon} \sum_i q_i n_{0,i} \exp(\frac{-q_i\phi}{k_B T}) \tag{6}$$

which can be used to calculate the counterion distribution around the PE. The PB is a mean-field theory. Mean-field theories simplify many-body contributions to an averaged field, thus reducing the system to a one-body problem. For PE solutions this means that nothing is described as point-like particles, but the electrostatic contributions of the counterions are averaged.

Although the PB theory works quite well with systems consisting of weak PEs and monovalent counterions[26] and further away from the PE[27], it has severe limitations. The basic PB equation does not take into account that counterions have volume that affects the overall system and that the counterions interact with each other. The

ions are not depicted as point charges, but with a mean-field approach. The result is that PB theory ignores many effects, such as charge correlations. However, the interactions between the PE and the counterions are in fact many-body type and localized[28]. The equation also assumes the PE to be an uniformly charged surface, and this assumption seems to fail in predicting ion condensation when the geometry of the PE differs from the initial assumption in the PB theory[29].

It has been shown by theoretical and computational methods that the Poisson-Boltzmann and Manning theories fail, when the ions are multivalent or their concentration is high enough[26,27,30–32]. The lack of charge correlations seem to result in excessively high predictions for the condensation when concentration or valency of the counterions grows[26]. MD simulations[29] also indicate the PB equation is a good approximation only if the PE really is uniformly charged and has cylindrical geometry[29].

Theoretical and numerical approaches[26,30,33] have revealed an interesting phenomenon, overcharging, i.e. charge reversal of the PE chain. It occurs when the charge of the PE chain is overcompensated by the counterions, and it increases with increasing PE charge per length[30]. PB theory or similar mean field approaches do not predict overcharging, due to the lack of charge correlations in the model.

Manning's theory does not consider electrostatic screening, which causes the failure of theory in the presence of multivalent ions, at high ionic strengths and with strong PEs[27,30,31]. Screening increases with ion valency[31]. In most systems, salt concentration does not affect the amount of condensing counterions[26]. However, the number of condensed ions is affected by change in screening length, which approaches the thickness of the condensed ion layer at high salt concentrations[26]. This effect of salt is not predicted by the PB theory.

Attempts to improve these widely employed theories have been made. The proposition by Deserno et al.[30] includes overcharging, but over-estimates it. Perel and Skhlovskii[27] correct existing theories by taking into account the special character of interactions at the vicinity of the PE. De et al.[23] have studied the effect of temperature, mixture composition and PE concentration on the counterion condensation phenomenon.

The effects of excluded volume effects have been recently studied by MD by Gordievskaya et al.[34]. They have established that the size of the counterions has a significant contribution to the behaviour of the PE[34]. Larger counterion size result in larger radius of gyration, an there is indication that collapse of PE chain in poor solvent might not take place or at least is altered with increasing counterion size[34]. The same research[34] also indicates that counterions of different size take different places at the PE chain. The conformation of the PE chain is affected by the counterion condensation. There are electrostatic interactions, both attractive and repulsive, between the charged species of PE solutions. Two similarly charged counterions repel each other, and can consequently restrain the relative movement of the parts of the chain the ions are condensed to. Due to these effects, counterions could be used to control the PE conformations, especially by adding multiple types of counterions. These effects become increasingly intriguing when multiple types of PEs are present in the same system.

In comparison to the described theories, particle based simulations typically take into account e.g volumes and many-body interactions. Particle simulations are parametrized with experimental or quantum mechanical data. The methods, such as MD simulations employing empirical force fields, usually aim to be well transferable, so they can be easily used to study many different systems, and they work well even for quite complex systems.

To conclude, the simple theories like Poisson-Boltzmann equation provide useful approximations of PE systems, but fail to describe many important features of these systems. Advances have been made, but still a thorough understanding of more complex systems is incomplete, and none of the suggested theories accounts for all of the features of this diverse and intriguing phenomenon. Particle simulations seem to be currently quite good solution for researching counterion condensation and comparing the effects in different systems. The importance of the role of the small ions in aqueous PE systems maintains the topic as a focus of research.

2.1.4 Solvent quality and polymer chain coil size

This chapter describes how solvent quality affects the balance between intrachain interactions and chain-solvent interactions of one polyelectrolyte chain, and presents the concepts and measures commonly used in polymeric sciences to assess the solvent quality for the polymer. These aspects are discussed in the results section of the thesis, as the focus is on the effect of solvent on PE interactions.

The balance between intrachain interactions and PE-solvent interactions determines the average chain coil size of single polymer chain in solution. Thus, the coil size can be used as a measure of solvent quality for the polyelectrolyte chain. As the chain coil size is strongly affected by the chemical structure of the polymer in question, measures of the chain packing need to be comparable from system to system. A polymer chain coil packing can vary from a fully extended chain to a tight, globular coil. Thus, one possible measure of the conformation of the chain is end-to-end distance of the PE chain, Nb, where N is the number of monomers of length b[35]. However, this quantity is not unambiguous due to the existence of highly branched PEs, in which determining two ends of the chain is not simple. Other measures are thus needed. The squared radius of gyration

$$R_g^2 = \frac{1}{N}\sum_i N(\mathbf{r}_i - \mathbf{r}_{cm})^2 \tag{7}$$

where N is the number of monomers, $\mathbf{r}_{cm}$ the centre of mass of the chain and $\mathbf{r}_i$ the position of i^{th} monomer, gives the mean squared distance of monomer i from the centre of the mass of the chain[35]. R_g is commonly used to describe the polymer chain coil size in solvent.

In addition to the length scales related to polymer chain coil size in solvent, measures of the volume of the chain are also used to describe and compare polymer sizes and polymeric solvent systems. Occupied volume of the chain NV_{mon} where N is the number of monomers and V_{mon} monomer volume, is the volume taken up by the polymer chain. Pervaded volume $V \approx R^3$, R being the radius of the polymer

coil, is the volume of the solution the polymer chain explores. The pervaded volume can thus be thought as the measure of the volume that the polymer is most likely occupying. It is considerably larger than the occupied volume for the chain, and most of the pervaded volume is filled by other molecular species of the solution, such as the solvent.

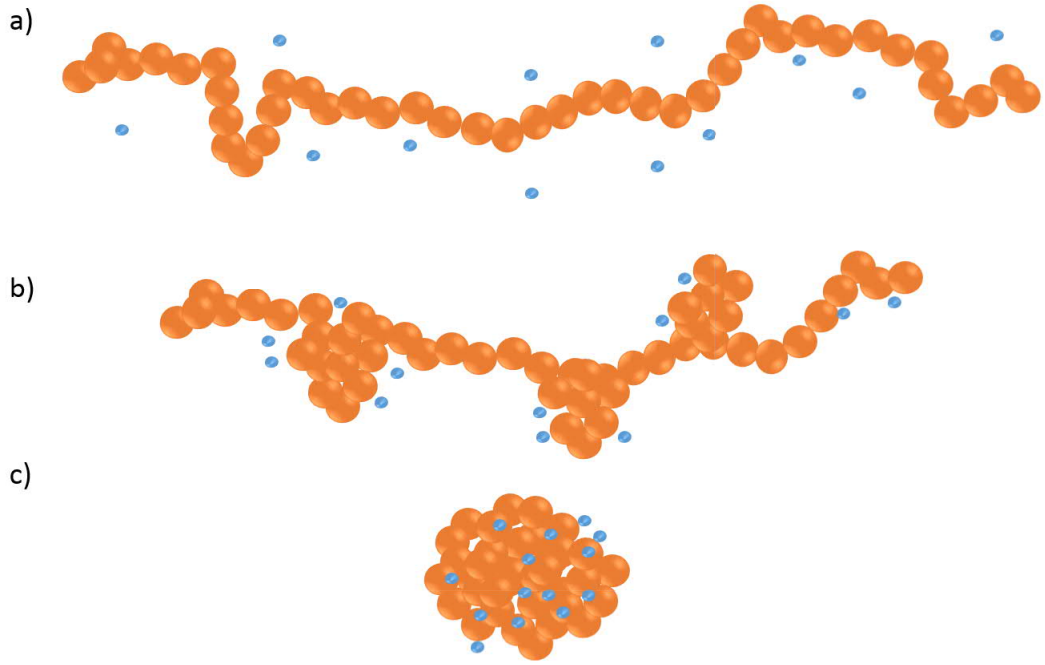

Figure 2: Polyelectrolyte coil packing with varying solvent-PE interactions. Orange beads represent monomers and blue beads counterions. In a good solvent, the chain is extended (a). In a poor solvent the intrachain attractions start to dominate, and the chain collapses first to a necklace (b), and in an even poorer solvent to a dense globule (c).

The radius of gyration R_g is useful when assessing effects of solvent properties on the chain packing of polymers. The better the solvent is for the PE backbone, the larger the radius of gyration. To distinguish between different solvent-PE interaction regimes, solvents in macromolecule solutions are commonly divided to three classes: good solvent, theta solvent and poor solvent. In a good solvent, the chain is fully extended, because polymer-solvent interactions are favourable, and R_g is high. When the solvent is poor for the polymer, the radius of gyration is small, because the chain will collapse into a conformation often called necklace[35]. The necklace consists of dense, globular parts with straight chains in between[35]. The necklace forms to avoid polymer-solvent contacts and maximize the polymer-polymer contacts[35]. With even poorer solvent conditions, the whole chain can collapse to one globular coil, which has very small end-to-end distance and R_g. Spherical form minimizes the solvent accessible area of the polymer. The described conformations are presented in Figure 2.

The theta solvent falls between the good and poor solvent regimes. In a theta

solvent the polymer chain acts like an ideal chain[36]. Ideal chain is a description of PE where conformation is independent of non-bonded monomer interactions, and the conformation is thus determined just by random walk[35]. In an ideal chain, the effects of the volume of the monomers on chain conformation are excluded, and the squared radius of gyration reduces to $R_g^2 = \frac{Nb}{6}$. In a good solvent the chain is more extended than an ideal chain, and in a poor solvent less extended.

Polyelectrolytes typically have both hydrophilic and hydrophobic groups. Consequently, a solvent is usually good for certain parts of the polymer, and poor for other parts[37]. Therefore, there are multiple types of polyelectrolyte-solvent interactions, even when only one kind of solvent is present. Also, real chains interact with each other via e.g. electrostatics, hydrogen bonding and hydrophobic interactions. Thus, for most systems, the ideal chain description is not valid, and more complicated descriptions have to be utilized to predict and reproduce the behaviour of PE chains.

The conformation of PEs is strongly affected by their charge, and the electrostatic screening of the system. When the charges of the PE chain are screened, for instance by added salt, the chain coil size is similar as for uncharged polymer. Usually PE chain does not collapse, due to the repulsive forces between its own monomers. The chain will thus adopt a rigid, extended conformation. The conformation of a single PE in solution thus depends both on the solvent quality and its charge density (charge/length)[38].

2.2 Multiple polyelectrolyte chains in solution

This chapter describes the behaviour of a solution containing multiple polyelectrolyte chains. The effect of concentration of polymer on the solution properties is described, as well as the association of polycations and polyanions.

2.2.1 Polymer concentration and rheology

Previous chapter addressed the behaviour of single PE chain in solution. When the solution contains multiple PE chains, depending on the concentration an conformation of the polymer, the chains can interact. Similarly charged chains repel each other, whereas the forces between oppositely charged PEs are attractive. Interactions between PE chains are affected by counterions and solvent, among other things.

With varying PE concentration, the properties of the PE solution vary. Two types of solutions can be distinguished: dilute and semidilute. These are presented in Figure 3 along with the so-called overlap volume fraction. In dilute solution, the polyelectrolyte volume fraction is below overlap volume fraction, and the PE chains are apart. The chains do not interact, and thus behave like single chains in solution. When the volume fraction achieves the overlap volume fraction, the chains start to come together forming a loose net-like structure. This is called semidilute solution. When the volume fraction of the PE increases further, the untangled polyelectrolyte net changes into a entangled, intertwined structure.

Overlap volume fraction can be written as

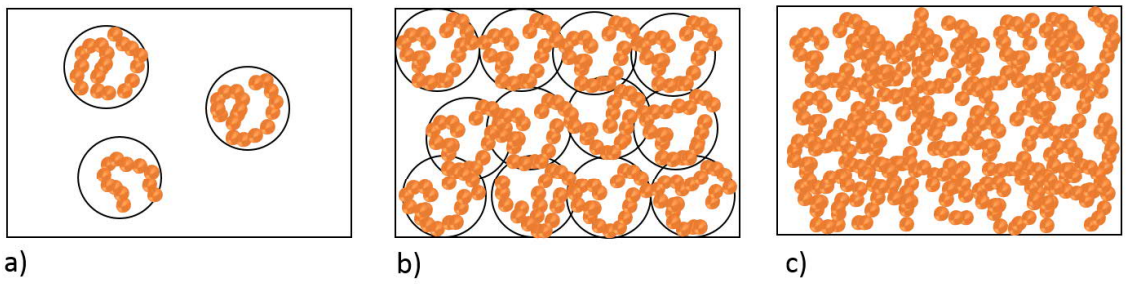

Figure 3: The concentration of the polymer affects the viscosity of polymer solution. In dilute solution (a), the chains do not interact with each other. At overlap volume fraction (b) the chains start to interact, and the solution crosses over to semidilute concentration (c). The rings around the chains approximate the pervaded volume.

$$\phi^* = \frac{NV_{mon}}{V} \tag{8}$$

and the corresponding concentration as

$$c^* = \frac{\rho N V_{mon}}{V} = \frac{M}{V N_A} \tag{9}$$

where ρ is the density of the solution, V_{mon} monomer volume, N_A Avogadro's number and V the solution volume. N is the number of the monomers ofdiameter b.

In a theta solvent, the overlap concentration reduces to

$$\phi^*_\theta = \frac{Nb^3}{R^3}\frac{1}{\sqrt{N}} \tag{10}$$

where R is the size of the chain, e.g. radius of gyration or end-to-end distance. The equation shows that only the lengths of the chains matter, as the chains act like ideal chains, and the volume effects are excluded, which simplifies the treatment of the system.

The interaction between PE chains is affected by the PE concentration of the solution. Dilute solutions are less viscous, and the PEs do not interact much with each other[35]. When the chains start to overlap, they begin to interact with each other. At high PE concentration, the mobility of chains is restricted due to steric effects, and the viscosity of the solution is increased[35]. In a dilute solution where there is only one type of PE and no salt, the PE cannot associate with other charged species. The interactions of interest are, therefore, intrachain interactions and chain-solvent interactions. These interactions and their balance determine the chain coil packing of the polyelectrolyte[35], as described in the previous chapter.

From the equations above, it is evident that the length of the chains affects the overlap concentration and, consequently, the viscosity as well; longer or more branched chains result in a more viscous solution, because there is less free solvent volume for the movement of the chains. Although the viscosity changes related to concentration and chain size are common to all macromolecular solutions, the rheology of PE solutions differs from that of uncharged polymers. For uncharged polymers, the viscosity of the solution is proportional to concentration of the polymer[19]. However, for PEs, the viscosity is proportional to the square root of the polymer concentration. This is called the Fuoss' law[39]. The special rheological behaviour is related to the conformation of PEs, which differs from the conformation of uncharged polymers due to the presence of charges in PE chains.

In PE solutions, the viscosity of the solution decreases with decreasing solvent quality[40]. This results from the change in the chain coil size. The viscosity of polymeric solutions originates from the intertwined network of the macromolecular chains. As the chains collapse to denser coil packing in poor solvent conditions, the radius of gyration and pervaded volume decrease, and the movement of the chains is less restricted than in good solvent[40].

2.2.2 Oppositely charged polyelectrolyte chains in solution

The previous chapters have provided basic background on the nature and behaviour of PE solutions. This thesis focuses on the interactions of a polycation and a polyanion in different solvent conditions. Thus, this section describes the association of PEs in solutions where both polycations and polyanions are present. Different theories on the energetics of this association process are discussed.

When a polycation and polyanion are present in the same solution, their charged groups can associate due to the attractive forces between them. The dissociation of two PE chains of opposite charges and their association is presented in Eq. 11. Both polyelectrolytes dissociate to either a polycation or a polyanion and oppositely charged counterions. The PEs then associate while the counterions remain in the solution.

$$\mathrm{Pol^+A^-} + \mathrm{Pol^-M^+} \rightleftharpoons \mathrm{Pol^-Pol^+} + \mathrm{A^-} + \mathrm{M^+} \tag{11}$$

The charges of the PE chain are compensated by pairing with oppositely charged species in the solution. There are two different kinds of PE-PE pairing: extrinsic an intrinsic pairing[41] (pictured in Fig. 4). Intrinsic pairing is the pairing of monomers of oppositely charged PEs, whereas extrinsic pairing refers to counterion-monomer-pairing[41]. The mode of charge compensation affects the properties of the complex[41,42]. Pairing between the oppositely charged polyelectrolytes and polyelectrolyte-counterion pairing are competing processes[24].

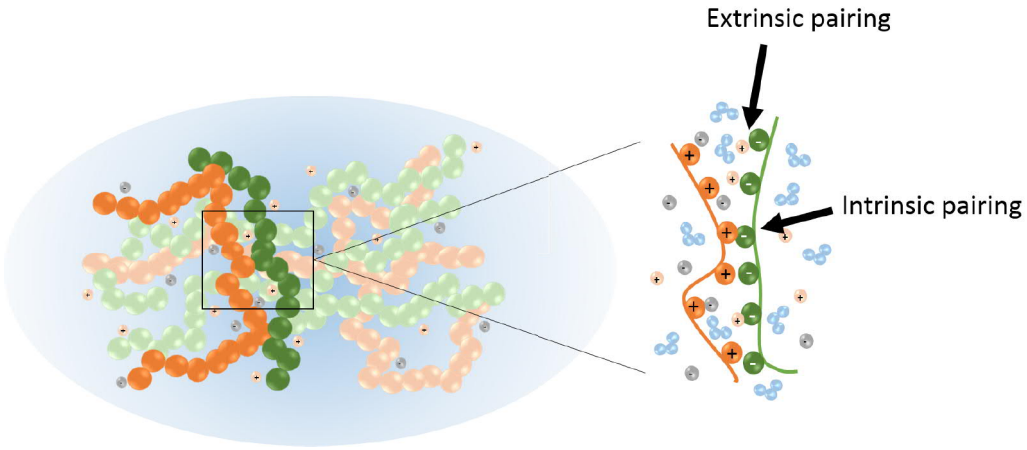

Figure 4: The charges of polyelectrolytes in polycation-polyanion solution can either associate with its counterions or with oppositely charged polyelectrolyte. The two pairing modes are called extrinsic and intrinsic pairing, respectively.

The energetic nature of the polycation-polyanion complexation has been researched for decades. The complexation occurs spontaneously, and is therefore exothermic[24]. Different solutions for the driving force have been presented[43–46]. Currently, the driving force of the complex formation is thought to consist of two main parts: enthalpic and entropic contributions[24,44]. The enthalpic part is the actual complex formation, i.e. the Coulombic interactions between the polycation

and the polyanion. The entropic contribution results from two sources. One of them is hydration shell removal, which occurs when solvent molecules move away from the PE during the association[24]. Other entropic contribution is the dissociation of the PE, where counterions are released to the solution[24]. In bulk solution the entropic contributions dominate[24]. The energetic contributions opposing the PE association are configurational entropy and steric constraints[47].

It has been proposed that the role of hydrophobic interactions on the PE complex formation is also significant[43]. Hydrophobic interactions are due to the often hydrocarbonous or otherwise hydrophobic backbone of the PE. The effect of hydrophobic interactions in the PE complexation results from the change in water entropy inflicted by these interactions[48]. The hydration shells of the PEs are thus affected by the hydrophobic interactions, and the hydration shell structure in turn greatly affects the interaction of PEs.

Biesheuvel et al.[46] have proposed that the mechanism for the complexation of oppositely charged PEs results from the decrease of electrostatic free energy when the oppositely charged monomers associate. The study[46] concludes that this decrease is greater than the increase in free energy that originates from conformation changes and mixing related to the complexation process. Biesheuvel et al.[46] have compared this approach to experiments, and have found that they correspond qualitatively.

Castelnovo and Joanny[45] have also made an approach similar to that of Biesheuvel et al[46]. Usually a mixture of two different polymers separates due to backbone-backbone interactions. However, both Biesheuvel[46] and Castelnovo[45] have concluded that the enthalpic mixing terms are overcome by the entropy that results from the counterion release. When the counterions move in both phases, the entropy stays higher[45]. The Castelnovo theory fails when the charge densities of the PEs are high, although in many cases it gives a good prediction of the association and is in line with other theories.

Langevin dynamics simulations by Ou and Muthukumar[49] indicate that the driving force for the PE association is different for weak and strong PEs. The study suggests that in a weak system the association process is driven by the attractive Coulombic interactions between the opposite charges, and in strong systems by the decrease in counterion entropy, as described by other theories above.

The theories of the driving force and energetic contributions of PE complexation have evolved, but the exact nature of this process still remains unconfirmed. It is nevertheless widely accepted that the two main contributions are enthalpic and entropic terms, mainly originating from polycation-polyanion association and counterion release, respectively.

Solvent affects the energetics of the PE association. It has an influence on the magnitude of the electrostatic interactions through its dielectric constant, i.e. affects the enthalpy. In addition to this, the solvent also affects the entropy of the system, especially in the case of binary solvent where one of the components is water. The hydrogen binding network of the water is changed by the additional solvent component, and this change in the system entropy affects the interactions of the PEs.

3 Polyelectrolyte assemblies

Polyelectrolytes tend to form different assemblies in polar solvents, when oppositely charged groups associate. The chapter discusses the formation conditions, behaviour and touches briefly the applications of two main types of polyelectrolyte assemblies, PE complexes and multilayers. The macroscopic properties of the assemblies are strongly affected by amount and quality of solvent. This thesis research aims to contribute to the development of these materials by providing information of the effect of solvent on polycation-polyanion interactions. Thus, the focus of this chapter is the role of solvent on the macroscopic-level behaviour of the materials, and special attention is given to the PEs and solvents studied in this research.

3.1 Polyelectrolyte complexes and multilayers

Being charged molecules, PEs can associate and form complexes with PEs of opposite charge, and other charged species, such as ions, molecules and surfaces. Positively and negatively charged PEs are called polycations and polyanions, respectively. When both polyanions and polycations are present in the same solution, they form polyelectrolyte assemblies with different three-dimensional morphologies due to the attractive forces between opposite charges[15,50]. The properties of these assemblies, such as the morphology, degree of organization, mechanical and physical properties depend on the characteristics of the PEs and the solvent. Temperature, pH and addition of salt also have an effect, among other things. The most important properties of the PEs affecting their assembly behaviour are molecular weight and charge density of the chain.

Polyelectrolyte (PECs) complexes are spontaneously forming three-dimensional PE structures[51,52]. They have potential in various biomedical and medical applications[51,53]. PECs are built by electrostatic forces between polycation and polyanion, and the formation is driven by a decrease in the total electrostatic free energy of the system[47,51]. Polyelectrolyte complexes can include more than two different polyelectrolytes. However, in the presence of three or more PEs (when at least one of them is of opposite charge compared to the others), selective complexification generally occurs.[51] Different combinations of polycations and polyanions result in different interaction strengths. Water and ions in the PE assembly have an effect on the interaction strengths[52].

PE multilayers (PEMs) consist of alternating layers of polycations and polyanions. Figure 5 shows the assembly and simplified structure of a PEC. The process of multilayer formation is called layer-by-layer assembly (LbL), but this term extends to all multilayers fabricated by this technique, not just the ones consisting of polyelectrolytes. The production of PEMs is achieved with successive deposition cycles, where every other cycle is polyanion and every other polycation. The layers are deposited on a substrate of choice from aqueous solution. PEMs can be thought as a special, highly organised subgroup of PECs. In reality, the layers of PEMs are not well-defined like in Figure 5, but the layers rather interpenetrate into each other. The film thickness can be regulated by adjusting the number of the layers or level of

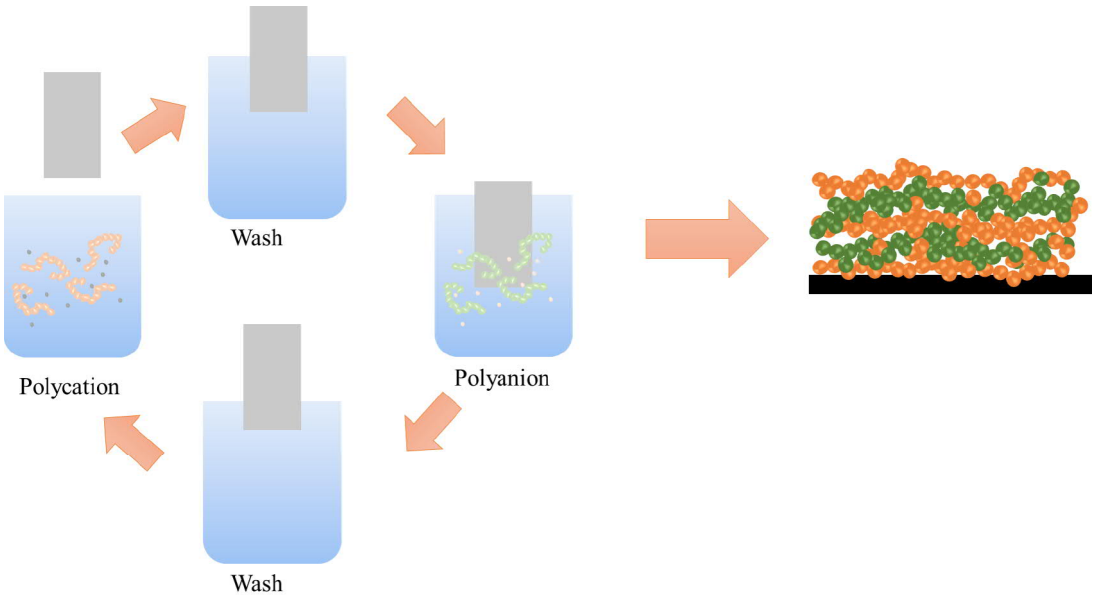

Figure 5: Layer-by-layer assembly of a polyelectrolyte multilayer consisting of polycations and polyanions, which are represented by the orange and blue chains, respectively. During the layer-by-layer process cycle, the substrate is alternately immersed to polycation and polyanion solutions with a rinsing between. The number of deposition cycles determines the amount of layers in the resulting membrane.

hydration of the multilayer assembly. The latter can be achieved for instance with increased humidity or tailored salt concentration[54].

The association process between oppositely charged PEs can result in soluble complexes or dense phases[47,55]. When complexation results in charge neutrality, the formed complexes often form dense phases[47]. Formation of soluble complexes is nevertheless possible, and occurs typically at high ionic strengths[47], when the PEs are more loosely associated.

Coacervates are colloidal droplets formed by liquid-liquid phase separation. Experimental and theoretical work are not yet connected well enough, additional work in theoretical approaches is required to understand the complex behaviour of these assemblies[55]. Coacervates are not discussed in detail here, due to their complexity and the difficulty of defining it and distinguishing it from the other described assemblies.

As described previously, there is a multitude of factors that influence PE-PE interactions. Variety of factors changes the cross-linking between PEs. In consequence, these factors, such as solvent quality[5], pH[4], deposition temperature[56] and ionic strength[6] have an effect on the complex formation and growth process of the PEMs and PECs. The properties of the PE, e.g. molecular weight, charge density, chain architecture and chemistry of the PE[57] are also significant. By changing these variables, the molecular-level structure can be tuned[24]. This offers a possibility to adjust the properties of the resulting PECs and PEMs, including size, shape, surface roughness and permeability can be controlled[51]. Due to this very special tuning possibility, PEMs and PECs have a vast variety of possible applications, including coatings, membranes with tunable permeability, drug delivery systems, and sensors[58]. The tuning can be done before or after preparation[24]. Also, substrate geometry is not restricted, although usually plates, small particles, and capsules are used[24].

The systems of interest in this study, PSS/PDADMA systems, have been studied experimentally very widely. Special interest has been on the role of salt on the properties of PEMs and PECs[6–8,59,60]. The dynamics of water and swelling properties in water have been an interest as well[7,8,61]. In addition to these, the effects of temperature[56,58] and molecular weight[62] on the properties and growth of PE assemblies have been studied.

Generally, salt affects the association of PEs, and thus the properties of PECs and PEMs. It has been shown experimentally that PECs do not form and existing complexes fall apart when the salt concentration exceeds a critical level[63,64]. Calorimetric measurements have shown that complex formation process becomes endothermic when the salt concentration is high[65,66]. When studying the effect of salt on PEMs, it has been observed that larger amount of salt or more hydrophobic salt results in thicker films, i.e., the layers from one deposition cycle are thicker than one monolayer[56]. The addition of salt has an effect on the growth rate of PEMs[8,24]. The growth of PSS/PDADMA multilayers is linear at low salt concentrations, but becomes exponential when salt concentration is increased[8,24].

The interactions of PE assemblies and salt are also closely related to the behaviour of water in the system. More hydrophilic PEMs are easier to dope with salt, which results in weaker complexes[56]. Salt also affects the degree of hydration of PE assemblies, i.e. the water content of the assemblies[56]. These observations demonstrate

that the effects of salt and solvent are coupled. However, as the effect of different salts or salt concentrations is not the focus of this thesis, salt effects will not be discussed in detail.

3.2 Effect of solvent on polyelectrolyte assemblies

The aim of this thesis is to understand how ethanol and urea affect interaction of PSS and PDADMA at microscopic level. The molecular level effects of these additives are assumed to produce also macroscopic level changes in PE materials. This chapter will thus briefly describe the so far observed effects and mechanisms of the solvent effects on PE assemblies. The focus will be on the materials relevant to this research, namely PSS and PDADMA, and effects of low-polarity solvents, such as ethanol.

When a polyelectrolyte assembly is completely dry, it is a brittle solid[15]. Water, the most utilised solvent, plasticizes PE assemblies[15] and solvates PE chains. The response of PEMs to the increasing water content differs from that of uncharged polymers[54]. For example, the changes in mechanical properties induced by increasing water content are significantly greater for PEMs than uncharged polymer films[54].

In macromolecular systems, water is not just a bulk solvent with homogeneous properties all over the solution. The water hydrogen bonding network is disrupted near interfaces, such as a surface of a macromolecule. As a consequence of this disruption, the behaviour of water depends greatly on the distance from the solute. Two main types of water can be distinguished in PE solutions by their translational motion compared to the solute: Bound water and bulk water[67]. The motion of bound water is strongly coupled to the motion of solute and bulk water is not affected by the solute[67]. Bound water forms the so-called hydration layer, the water in the proximity of the solute and affected by it. The water molecules closest to the PE interact with the PE e.g. via hydrogen bonding, and the water molecules that cannot bind with the PE hydrogen bond with the waters closer to the PE. Hydrogen bonding lifetime kinetics in the hydration layer differ from those of the bulk water[68].

Water has high dipole moment and dielectric constant. Liquid water is a web of water molecules interlinked by hydrogen bonds. These characteristics affect its solvation ability and dynamics in different systems. Thus, in PE solution, when some or all of the water solvent is replaced with a lower polarity solvent with different hydrogen bonding ability, the solvent-PE interactions will drastically change. The dielectric constant decreases when the polarity of the solvent decreases[5]. Because at least the charge groups of the PE are hydrophilic, the solvation of the PE comes less favourable when the solvent is more hydrophobic[69]. Therefore, ethanol is poorer solvent for the PEs than water[69].

In addition to the interactions between the solvent and the solutes, the interactions between solvent components strongly affect the system behaviour when two or more solvent components are present. For instance, in ethanol-water mixtures the two components might separate, resulting in a formation of clusters[17]. Ethanol and water interact through hydrophobic interactions and hydrogen bonding, and the balance between these two types of interactions determines the formation of clusters[17].

Experimental work on PSS/PDADMA multilayers in water-ethanol mixtures[5]

has revealed that the thickness of the deposited layers increases with increasing ethanol concentration of the PE solutions. It has also been observed that PEMs fully submerged in 100% ethanol are less swollen than those submerged in pure water[70]. PEMs in ethanol are still thicker than dry ones, so the PEMs do have a small ethanol uptake[70]. The decreased electrostatic screening and increased hydrophobicity of ethanol mixtures compared to water seems to result in stronger PE association, and decreased swelling of PSS-PDADMA PEMs[5,70].

There has been very little research on the effect of urea on PEs. The effect of urea has been studied on weak PE gels[71,72]. The results indicate that urea increases pH-induced swelling behaviour of the gels. This is thought to be caused by the disruption of hydrogen bonding between the PEs and water. Thus, the net-like gel structure stabilized by the hydrogen bonds is loosened by urea.

To summarize, the solvent has a major effect on the physical properties of PE assemblies: The degree of hydration regulates the stiffness of the assemblies, and the addition of low-polarity solvents can decrease the hydration and induce contraction of PEMs. In addition to these changes in the mechanical properties, the effect of water on the thermal properties of PE materials is significant. This will be discussed in the following chapter.

3.3 Thermal behaviour of polyelectrolyte assemblies

In this section, the thermal responses of polyelectrolyte assemblies are discussed. Review of experimental and computational research is included. The section is especially concentrated on the role of solvent in the thermal behaviour of these structures for its relevance to the thesis topic.

The properties of PE assemblies depend on temperature. Generally, viscosities of PE solutions decrease with increasing temperatures[56]. Mobility of chains increases, and the PE structure softens. Temperature affects also the growth of PEMs; higher temperature results in thicker PE bilayers, and linear growth can change to non-linear[56]. Increasing temperature results in less cross-linking between PEs, and the structures can reorganize to new configurations more easily. The effects of increasing temperature are similar to increasing ionic strength, because both of them weaken the polycation-polyanion interactions.

It has been shown experimentally that a reversible, glass-transition-like thermal transition occurs in PECs[73] and PEMs[74]. It is called glass-transition-like due to its character: when raising the temperature over a certain limit, there is a sudden change in the softening. The transition is a result of an increase in the PE mobility. This increase can derive from a variety of sources.[13,60,73,74]

The role of water, or solvent in general, in this thermal transition is undoubtedly substantial. Modulated differential scanning calorimetry (MDSC) measurements have shown that water molecules are bound to the PE even at high temperatures, where binding weakens[13]. Higher water mobility inducts transition. When the mobility of water increases, the water-PE-binding loosens, and, in consequence, the PE assembly softens.[13,60] Simulations and experiments (MDSC studies) suggest that the transition is initiated by water-PE interactions[13]

There are indications that the transition occurs in water, whereas it does not happen in alcohols (1-propanol, n-butanol, ethylene glycol were studied)[13]. Therefore, the hydrogen bonding ability of the solvent could relate with the occurrence of the transition. In addition to the quality of the solvent, the amount of it has an effect on the transition as well. Higher degree of hydration results in lower transition temperature[60].

As described, increasing water mobility appears to correlate with the occurrence of the described glass-transition-like thermal transition[13,60]. However, there are indications that increasing salt concentration causes a decrease in water mobility while still accelerates the thermal transition[60]. Increasing salt concentration results in decrease of PSS/PDADMA interactions. This means that the PE mobility increases. However, salt also changes water dynamics by binding water rather strongly in comparison to water-water H-bonding and PE-water bonding.[60]

Even with these experimental and computational efforts, microscopic description of the factors leading to the previously described thermal transition does not exist. The solvent-PE-interactions as well as PE-PE interactions are the key to understanding this interesting phenomenon. The described research on thermal properties raises interest of the water's role and, in general, its behaviour in systems including PE complexes.

4 Materials modelling

Experimental work is the basis of natural sciences. However, some systems and properties are extremely hard to study experimentally, even with the most sophisticated equipment. Thus, to extend materials research beyond the capabilities of experimental work, a vast variety of modelling methods have been developed. This section provides a brief overview of materials modelling and involved techniques, focusing on those used in this work.

4.1 Materials modelling in general

Physics based models of materials are created to deepen the understanding of the behaviour of materials. These models are often computational. The highest level of detail in materials modelling is obtained by quantum mechanical methods. Quantum mechanical modelling operates on atomistic scale, accounting explicitly for electrons. Depending on the method, the system sizes are limited to approximately 100-3000 atoms[75], time scales to tens of picoseconds.

Often larger systems or the system changes at larger time scales are of interest. Molecular dynamics (MD) encompasses a variety of methods that are often employed to study the dynamics of systems. When using quantum mechanical MD, the simulation times are typically in the order of picoseconds. Large systems cannot be simulated with quantum mechanical techniques due to extremely high computational cost, as the number of electrons grows very quickly with increasing atom count.

When the number of atoms reaches thousands, quantum mechanical calculations start to be too costly. Thus, when the studied system is larger, but individual atoms or molecules are of interest, classical molecular mechanics are employed. Molecular mechanics do not use quantum mechanical equations, but empirical force fields to describe the materials response. Empirical force fields are sets of functions and parameters adjusted to reproduce the results of quantum mechanical equations or experiments, without treating electrons explicitly. These methods can be used for upto 10^4 particles[76].

The two main techniques in classical molecular mechanics are classical MD and Monte Carlo (MC)[77]. In MC there is no temporal relationship between the system configurations[77]. It samples randomly possible system configurations. Low-energy configurations are then found from the calculated configurations using probabilistic methods. Monte Carlo suits well for calculation of thermodynamic averages.

Unlike MC, MD allows the observation of time dependence of system properties, as configurations are calculated as consecutive time steps[77]. An MD simulation forms a time evolution trajectory of particle positions, movements and interactions for a certain time period with a chosen set of parameters and algorithms[77]. The system defined by initial configuration, which specifies e.g. bonds between atoms, crystallography, charges. These initial configurations are often created using data obtained from experiments and/or theory. The particles are usually placed inside a simulation box.

Because MD provides a molecular-level description of moving and interacting

chemical species, it suits well for observing behaviour of systems at molecular level and addressing chemistry-related problems[77]. MD can provide information of system configurations, such as molecular conformations and complex formation. However, as systems of interest often include large molecular assemblies and complex structures, such as proteins, polymers and micelles, the system size tends to be quite large, and there is often a compromise to be made between accuracy and computational cost. Consequently, there are different possibilities for the detail level in molecular mechanics simulations. The choice of dynamic modelling method is determined by the desired time and length scales. With higher level of detail, both the possible time and length scales decrease, due to computational cost. Either all atoms can be included (atomistic simulations), or some groups of atoms can be handled as pseudo-atoms. The latter way is used in coarse-grained models. There are various models with different levels of detail: The most detailed coarse-grained options reduce only hydrogen atoms linked to a neighbouring heavy atom to a single site. Other schemes reduce multiple heavy atoms or functional group, or even an entire molecule to a single site. The choice of the model depends on the studied characteristics of the system, and the system size. Coarse-grained models do not describe the system with all chemical details[78]. This is useful when the interactions of interest are not very localized, and the desired time and length scales are large[78]. With the help of coarse-grained models, simulation durations can reach microseconds with reasonable computational cost[78,79].

When the molecular-level behaviour is not of interest, mesoscopic and macroscopic models are used. These models can e.g. give macroscopic properties of the material, such as time evolution of multi-phase structures, for example polymer blends or block copolymers[78–80]. So-called continuum methods can be used to model thermodynamical and physical properties of bulk materials. These models can provide information of e.g. fluid dynamics, elasticity of solids[79]. Time scales for these systems are around $10^{-8} - 10^{-4}$ s, and length scales from micrometer scale to hundreds of meters[79].

In this thesis, all simulations are performed using molecular dynamics with an atomistic detail force-field, because the specific chemistry of the interactions in the system are of special interest. Next chapter is dedicated to classical MD techniques, with focus on the methods employed in this thesis.

4.2 Molecular dynamics

This section provides an overview of the constituents of classical molecular dynamics models for atomistic detail simulations.

4.2.1 Force fields

Molecular dynamics (MD) methods for molecular and atomic level modelling are one way to model time development of a particle system. Classical MD is an empirical force field method. MD is a method that is used widely to obtain structural and mechanical information of various systems. It has been employed widely to, e.g. biomolecular simulations, where the system size is quite large compared to quantum

mechanical methods.

A molecular dynamics simulation provides information about movement and interactions of particles as functions of time. The forces between the particles are calculated based on empirical force field[77,81]. Force fields consist of a mathematical expression of the interaction energy in the system with parameters, which are fitted to reproduce data obtained experimentally and via quantum mechanical modelling. Force fields allow the calculation of the energy of the system using atomic positions while ignoring quantum effects, i.e. the electronic structures of the particles present, which reduces computational cost compared to quantum mechanical methods. Force fields combine electrons and the nucleus to an atomic description, and the electronic effects are thus accounted for as an average over the whole atom.

Force fields are generally parametrized and built to produce description of as many systems as possible. In other words, force fields should be transferable. Although force fields usually do work for various different systems, there is no single universal force field that would produce accurate results for all possible systems. Consequently, the choice of the force field should be done carefully, and the obtained results evaluated with respect to the methodology used. In this study, the Optimized Potentials for Liquid Simulations (OPLS) force field is used for all simulations. More precisely, the all-atom OPLS (OPLS-aa), which includes all atoms[82] is used. OPLS-aa is widely applicable and well verified for liquid systems, which is the reason it was used here. It has been parametrised for organic solvents, proteins etc., which makes it extremely suitable for the systems in this thesis work.

Force field consists of a functional form and parameters. The functional form is the mathematical representation of the force field. The parametrization provides the parameter values that are inserted to the functional form. The functional form of OPLS-aa[83] is presented below as Equations 12 - 16. Equation

$$E_{tot} = E_{bonds} + E_{angles} + E_{dihedrals} + E_{non-bonded} \tag{12}$$

is a general functional form that is used for the energy in multiple force fields. It shows that force field is a sum of bonded terms and non-bonded terms. In it,

$$E_{bond} = \sum_{bonds} K_r(r - r_{eq})^2 \tag{13}$$

where K_r is the spring constant for the vibrating bond, r the length of the bond at certain moment and r_{eq} the equilibrium length of the bond, is the term for bond stretching,

$$E_{angle} = \sum_{angles} K_\theta(\theta - \theta_{eq})^2 \tag{14}$$

where K_θ is the spring constant for the bending angle, θ the angle at certain moment and θ_{eq} the equilibrium angle, describes angle bending energetic cost,

$$E_{dihedrals} = \sum_{dihedrals} (\frac{V_1}{2}[1 + cos(\phi + f1)] + \frac{V_2}{2}[1 - cos(2\phi + f2)] + \frac{V_1}{3}[1 + cos(3\phi + f3)]) \tag{15}$$

where V_1, V_2 and V_3 are torsional terms, ϕ measured dihedral angle and $f1$, $f2$ and $f3$ phase angles, represents dihedrals, and

$$E_{nb} = \sum_{i<j} \left(\frac{q_i q_j}{r_{ij}} + \frac{A_{ij}}{r_{ij}^{12}} - \frac{C_{ij}}{r_{ij}^{6}}\right) \tag{16}$$

where q_i and q_j are the charges of interacting particles i and j at a distance r_{ij}, $A_{ij} = \epsilon r_{ij}^{12}$ and $C_{ij} = \epsilon r_{ij}^{6}$ where ϵ is the depth of the potential well, accounts for non-bonded interactions, namely electrostatic and van der Waals energies. The physical meanings behind these components of the force field are demonstrated in Figure 6. The bond stretching term Eq. 13 describes the lengthening and shortening of a bond between two atoms. The angle bending term accounts for changes in the angle between two bonds. Dihedrals and torsional terms are for the rigidity of the bonds, to account for conformations in molecules that include at least four atoms.

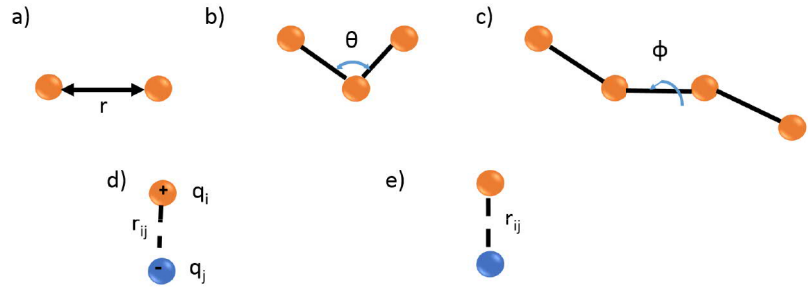

Figure 6: Key components of MD force fields consist of three bonded interactions which are bond stretching (a), angle bending (b) and torsion/dihedral (c), and non-bonded interactions: electrostatic interactions (d) and van der Waals forces (e). See equations 13 - 16 Adapted from[77].

Experimental properties of liquids have been used for parametrization of the OPLS-aa force field[83] In OPLS-aa, the charges are chosen so that the resulting interaction energies and geometries are in accordance with quantum mechanical calculations[84]. Thermodynamics and interactions in liquids correlate well with experiments[85]. The OPLS-aa force field was developed for organic and biomolecular liquid systems[83]. The parameters have been adapted for e.g proteins[83] in water and for various organic liquids[83]. Thus, it can be expected to suit quite well for PEs in water-based solutions. It has been utilized to simulate PEs, and it seems to agree well with experiments with e.g. basic physical properties of PE complex solutions[86], water content of PE bilayer[87] and thermal softening behaviour[88]. OPLS-aa appears to be an excellent force field option for the simulation PE systems, and is therefore utilized in this thesis.

There are various water models available. Not all models are compatible with all force fields. In this study, TIP4P, an explicit water model was used. TIP4P water model[89] includes a fourth particle in addition to the three atoms in water molecule. This adds the computational cost, but improves the accuracy of the model in terms of improved water phase diagram reproduction and more accurate dielectric constant compared to simpler models such as TIP3P and SPC[84].

4.2.2 Equation of motion and its numerical integration

In addition to the system energy produced by the force field, the particle motions need to be described. Classical mechanics are used to calculate motion of particles in the system. Newtonian equations are integrated numerically to approximate the behaviour of moving and interacting particles.[90] MD simulation forms a trajectory that has positions and velocities of particles as functions of time. The trajectory comes from Newton's second law

$$F = ma \tag{17}$$

where F is force, m mass and a acceleration. Second law can be transformed to a differential equation

$$\frac{d^2x_i}{dt^2} = \frac{F_{xi}}{m_i} \tag{18}$$

which is integrated numerically to form the trajectory using so-called finite difference methods[77]. These methods rely on numerical integration by splitting the integral to smaller steps that are separated by the time step Δt[77]. The base of these integrating techniques is that dynamic properties of particles in the system can be approximated as Taylor series expansions, i.e. as sums of derivates of the studied property around time t. For example, for velocity this means

$$\mathbf{v}(t + \Delta t) = \mathbf{v}(t) + \Delta t\mathbf{a}(t) + \frac{1}{2}\Delta t^2\mathbf{b}(t) + \frac{1}{6}\Delta t^3\mathbf{c}(t) + ... \tag{19}$$

where $\mathbf{v}$ is the velocity, and $\mathbf{a}$ acceleration of the particle. These are also the first and second derivative of the position of the particle in question and $\mathbf{b}$ is the third derivative. The t is the initial time and Δt the time step[77].

This study uses leap-frog algorithm for integration of the equation of motion (Eg. 18):

$$v_n(t + \frac{1}{2}\Delta t) = v_n(t - \frac{1}{2}\Delta t) + \frac{\Delta t}{m}F_n(t) \tag{20}$$

$$r_n(t + \Delta t) = r_n(t) + \Delta t v_n(t + \frac{1}{2}\Delta t) \tag{21}$$

$$v_n(t) = tv_n(t + \frac{1}{2}\Delta t) + v_n(t - \frac{1}{2}\Delta t) \tag{22}$$

where m is the mass, $F_n(t)$ the force, $r_n(t)$ and $r_n(t + \Delta t)$ positions for particle n at times t and $(t + \Delta t)$, respectively. Equation 22 allows the calculation of the velocities at time t, as the algorithm (Eq. 20 and 21) contains the velocity $\frac{1}{2}\Delta t$ ahead or behind the position t. The leap-frog algorithm[91] is a numerical integration method commonly employed in MD simulations to integrate equation of motion (eq. 18). The leap-frog method uses continuous potentials. The calculated states of the system are separated by the time step Δt. During the time step, forces are kept constant. Therefore, choosing an appropriate time step is extremely crucial for the simulation.

A too large time step will cause loss of important system features, but too small step size will result in computationally costly simulations.

The integration of the equations of motion results in combinations of coordinates and momenta of all the particles of the system. One combination corresponds to one system configuration. The configuration can be thought as points in space. This space formed by all the possible configurations for a simulation system is called phase space[77]. Usually, it is impossible to sample all possible points of the phase space due to large system sizes and finite simulation times[77]. Thus, the results depend, to certain extent, of the initial configuration[77].

To enable efficient probing of the phase space, the starting configuration of the simulation has to be reasonable. So-called minimisation algorithms optimise the structure and position of the particles in the modelled system prior to the actual simulation. Many of these algorithms are based on calculating derivates of the energy, as the first derivative points to the direction of the minimum on the so-called potential energy surface, which presents the energy as a function of the coordinates. This thesis uses for energy minimization of the initial configuration a widely employed derivative method, the steepest descent method. The steepest descent method results in the particles moving along the steepest gradient, i.e. the directional first-order derivative towards a local energy minimum.

4.2.3 Periodic boundary conditions

As it is practically impossible to simulate infinitely large systems, all materials modelling simulations have to have some kind of boundaries, and the behaviour of particles near the boundary has to be defined as well. Typically, a simulation box defines the boundaries for the simulated system. These boundaries can be impenetrable by the particles, which typically means that the particles are reflected from the walls of the simulation box. An alternative for hard, reflective boundaries are periodic boundary conditions (PBC). PBC takes the defined simulation box as a unit cell. This unit cell is then surrounded by periodic repetitions of itself called images. In practice this means that when a particle crosses the boundary of the simulation box, it enters the same simulation box on the other side of the box. PBC is depicted in the Fig. 7 below.

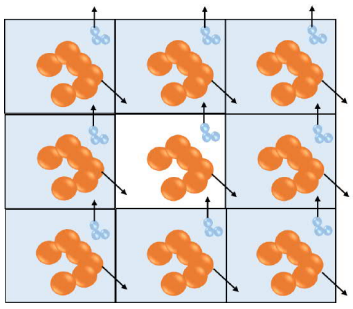

Figure 7: Periodic boundary conditions in two dimensions. Unit cell in the centre, surrounded by the periodic images.

Periodic boundary conditions allow modelling of bulk properties without increasing the simulation box size and computational costs substantially. In atomistic detail simulations, the chosen system size is usually quite small to minimize computational cost, usually in the order of nanometres.

However, for instance when studying phenomena related to e.g. large macromolecules, aggregates or complexes, the system should be large enough to be able to reproduce the phenomena related to larger structures. The same problem is faced with virtually all other systems. In MD, the dimensions of the simulation box are often in the order of nanometres. In a box of this size, if the boundaries are hard, impenetrable walls, the wall-collision frequency of the particles would be high. The system would be a description of the interface, and not of the bulk properties of the system in question. Therefore, PBC are normally utilized, and they are also employed in this thesis.

4.2.4 Electrostatics

In MD simulations, the computationally most costly part is the calculation of electrostatic interactions. Therefore, efficiency of the methods used for these calculations is of great significance. The Ewald summation method[92] allows to calculate interactions between particles in periodic systems. Perhaps the most widely used approach in molecular modelling for treating electrostatic interactions, there are different variations of this method. In this thesis, the particle mesh Ewald summation method (PME) is used. PME is a more efficient, mesh-based implementation of the Ewald method. The Ewald summation methods relies on splitting the summation of the Coulombic interactions into a short-range and a long-range component[92]. Alternatives to accurate determination of electrostatic interactions include cell multipole method and reaction field method, which are not covered in this thesis[77].

4.2.5 Temperature and pressure control

The direct result of the previously described numerical integration of the equation of motion is that the particles in the molecular dynamics simulation follow the so-called microcanonical ensemble NVE. In practice it means that during the simulation the number of particles N, system volume V and the system total energy E are constant. However, in experimental studies, it is easier to control, for instance, temperature or pressure than the energy of the system. Thus, other ensembles such as NVT, where instead of the system energy the temperature T is constant, or NPT, where both the pressure P and the temperature are constants are used also in simulations to make them comparable to experiments. This study uses NPT, which is called the isothermal-isobaric ensemble. It makes the results easier to compare with experimental data. In order to achieve the NPT canonical ensemble instead of the microcanonical ensemble, additional algorithms are required to control the temperature and pressure in simulations. These algorithms, thermostat and barostat algorithms, are shortly presented focusing on those employed in this study.

Thermostat algorithms are utilised in MD simulations to control the system temperature. In this thesis, the V-rescale thermostat algorithm[93] is used. It is

an improved version of the Berendsen thermostat algorithm[94]. The Berendsen thermostat algorithm couples the system to an external bath with certain temperature, and rescales the particle velocities and thus the kinetic energy of the system toward the bath temperature[93].

To obtain the NPT ensemble, in addition to a thermostat algorithm, barostat algorithms are employed to control the system pressure. This study utilizes Parrinello-Rahman barostat algorithm[95]. The Parrinello-Rahman barostat algorithm allows the volume and shape of the simulation box to change[95]. The shape change allows simulation of solids, because phase changes to different crystallographic structures are not restricted by the barostat algorithm[95].

4.3 Modelling polymeric systems

As this thesis studies the interactions in polyelectrolyte solutions via numerical modelling methods, this chapter provides a brief overview of methods utilized to model polymeric materials. To provide more specific background for the simulations performed in this research, the focus is on the modelling of polymeric solutions and PEs. A short review of modelling methods utilized for the modelling of PSS/PDADMA systems is incorporated, as these PEs are the focus of the thesis.

As previously described, some models work at short time scales and small lengths scales, whereas others can describe well phenomena that occur at longer time scales and larger length scales. Therefore, the choice of the model can be straightforward, if only small or large scale is relevant in the system of interest. However, in PE systems, the presence of multiple time and length scales makes the choice of model challenging[96]. The significant length scales vary from the few nanometre long monomers to the chains consisting of thousands of monomers, reaching length at micrometre scale, and the macroscopic structures formed by the chains, for which the dimensions can reach centimetres[96].

Consequently, a variety of methods are required to capture the phenomena related to polymeric materials at different scales. Due to the large size of polymer molecules, quantum mechanical means are usually out of the question when modelling polymers. Thus, particle-based models, field-theoretic ones and continuum models are widely employed, as well as lattice models and polymer scaling theories. Continuum models allow the modelling of phenomena relevant to process engineering, e.g. flow of polymer melts[97]. Field-theoretic approaches are used to simulate bulk properties, such as densities[97].

Polymer scaling models employ the observation that many of the properties of polymer solutions depend on the chain length of the polymer. Extremely vast number of scaling laws exists. They are mathematical models that describe some property of polymeric solution, incorporating the number of monomers, as the property is scaled according to the chain length. Polymer scaling laws can be utilized to obtain approximations of thermodynamical properties and e.g. screening lengths in polymer solutions[98]. The scaling laws are usually applicable at certain solvent quality conditions and concentration region[98].

Lattice models describe polymer solutions as lattices. Each site in the lattice

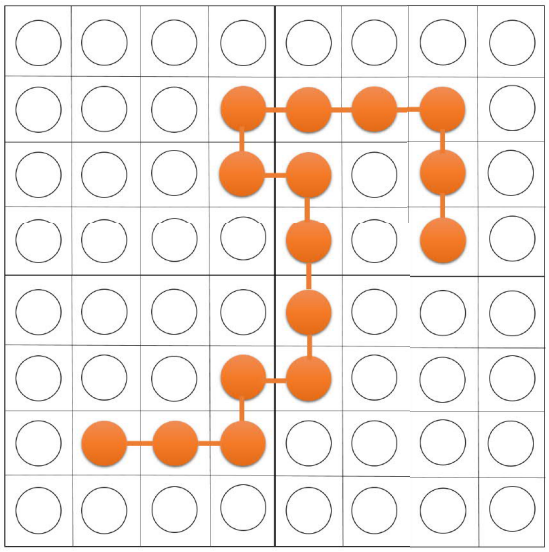

Figure 8: Lattice model of polymer in solution. Orange circles represent segments of polymer, unfilled circles solvent molecules.

is occupied either by a solvent molecule or a polymer segment[99] (Fig. 8). A widely utilized lattice model for the approximation of thermodynamical properties of polymeric solutions is Flory-Huggins theory[99].

Particle-based methods, such as previously mentioned classical MD and MC, provide information about molecular-level behaviour of polymeric systems[97,100]. The exact choice of method depends on the system and quantities/qualities to measure from it. MC provides information on thermodynamical properties of polymer solutions and melts[97], whereas MD is utilized in polymer modelling to study e.g. conformational changes, transport properties of melts,[97]. For the modelling of larger systems, united-atom force fields and coarse-grained models provide an option to reduce computational cost.

The PSS/PDADMA complexes and layers, the materials of interest also in this thesis, have previously been modelled mostly using atomistic classical MD with explicit solvent. Research topics have included PSS/PDADMA PEC formation, role of salt and water[86], role of surface charge on the formation of PEMs[87], role of water on interface of PSS-PDADMA bilayer and water[101], and water mobility in hydrated PSS-PDADMA complex at different salt concentrations[60]. In addition to the atomistic MD, a coarse-grained MARTINI method for PSS/PDADMA complexes has been presented[102]. Polyelectrolytes have some special features that affect the choice of the modelling method. Although empirical force-fields have not been parametrized for synthetic PEs, they seem to reproduce well-known properties of these materials quite well. Model agrees to some extent with atomistic models[102], but the method has not been widely adopted. Non-atomistic models, such as lattice methods, do not have chemical specificity, so they can be considered as general model for (a certain group) of PEs. Therefore, many methods can be used to predict and reproduce of the behaviour of PSS and PDADMA. Nonetheless, these methods are not discussed in detail as the method of choice in this thesis is atomistic classical MD.

5 Methods

The empirical research of the thesis consisted of simulations of individual chains of PSS and PDADMA in water and in the presence of ethanol and urea. This chapter presents the utilized numerical methods, studied systems, and the methods employed for the analysis of the obtained data.

5.1 Simulation methodology

The simulations of this thesis were all-atom simulations performed with the Gromacs 4.6.5 package[103]. OPLS-aa force field[104] was used in all simulations for the PEs, ions ethanol and urea, because it is optimised for liquid systems and successfully used in the modelling of polyelectrolytes[29]. PSS and PDADMA chain with Na^+ and Cl^- as counterions were examined. Water was modelled using the TIP4P water model[89]. It is one of the water models in compliance with the OPLS-aa force field, and it reproduces the properties of water better than TIP3P, which is another possible water model for OPLS-aa[84,89]. OPLS-aa parameters for urea[105] and ethanol[83] were utilized, PEs were parametrized like described in[29]. Periodic boundary conditions were used for all the systems to avoid interfacial effects at the edges of the box.

For the regulation of temperature and pressure, the V-rescale thermostat[93] and semi-isotropic Parinello-Rahman barostat were used[95]. For the thermostat, coupling constant of 0.1 ps and reference temperature of 300 K were used. Two thermocoupling groups were employed: water and ions and other. The latter thus included polyelectrolyte and the solvent additive. The coupling constant for the barostat was 1 ps and reference pressure 1 bar. The semi-isotropic barostat was set so that it lets the x and y dimensions of the box change, keeping the z constant. This method was chosen due to the stretched PE chains present in these simulations: the PE chain spanning the box in the z-direction needs to maintain its length.

The Particle Mesh Ewald summation method[106] was used to calculate the long-range electrostatics in the studied systems. It is a widely used, improved version of the Ewald method[92]. It is included in the Gromacs package. Short-range electrostatics and van der Waals cutoffs 1 nm. Bonds were constrained by the LINCS algorithm[107]. For the integration of equations of motion, leap-frog integration scheme with a 2 fs time step was used.

5.2 Studied systems

All the solvents were simulated without PEs to assure the validity of the chosen methods. The initial size of the cubic simulation box was 5 nm x 5 nm x 5.7 nm. The boxes were built by first defining the box dimensions and inserting desired number of the solvent additive molecules. Then water molecules were added.

First, energy minimization was performed for all systems using the steepest descent method. All the simulations were equilibrated for 200 ns and then simulated for another 200 ns. The simulation time was chosen to ensure that the fluctuations of solvent properties average out. The equilibration time was determined from the

dynamics of the solvent density fluctuations in solvent-only and in the single-PE-systems.

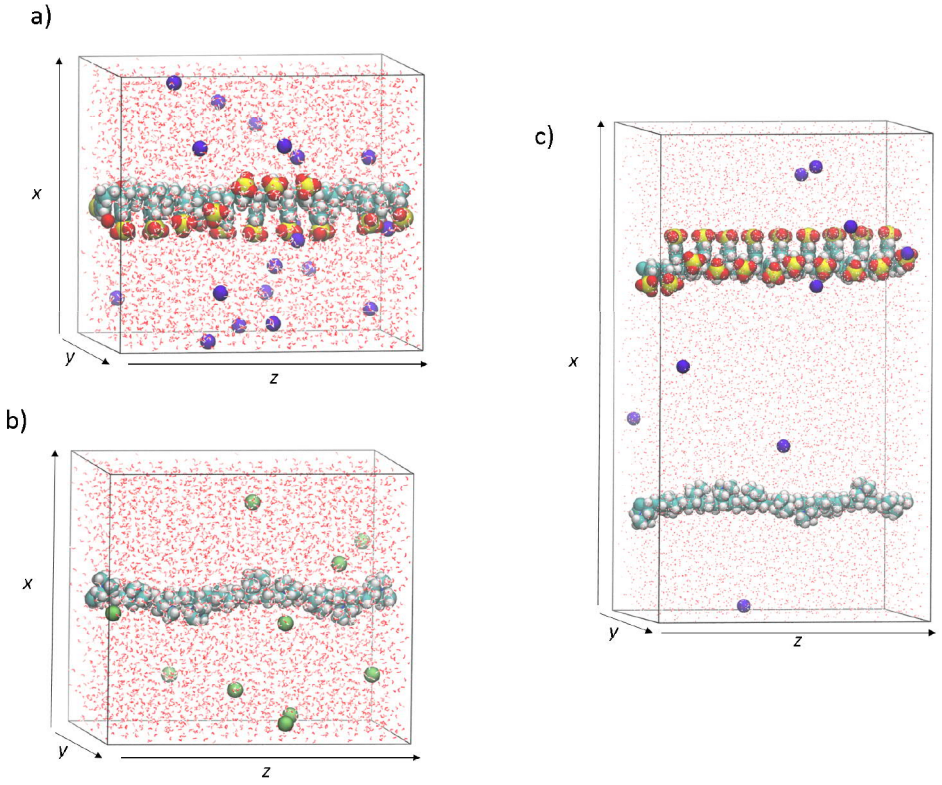

Figure 9: 10-monomer PDADMA chain a) and 20-monomer PSS chain (b) in water with counterions. Blue and green ions correspond to sodium and chloride ions, respectively. Box dimensions are 5 nm x 5 nm x 5.7 nm. c) PSS-cahin and PDADMA chain in water with 10 Na-ions in a 10 nm x 5 nm x 5.7 nm box.

The PE chains used in this study were 20 monomer long PSS and 10 monomer PDADMA chains (chemical structures in Fig. 1), because these chains are the same length. Both PEs were simulated individually in five different solvents systems: water, 10 wt% ethanol in water, 30 wt% ethanol in water, 10 wt% urea in water and 30 wt% urea in water. Counterions were added to obtain a zero net charge for the systems. For PSS systems, 20 sodium ions were added and for PDADMA systems 10 chloride ions. The initial size of the cubic simulation box was 5 nm x 5 nm x 5.7 nm. The box size was chosen so that the polyelectrolyte chains do not affect the whole solvent volume, and z-axis dimension was the length of the PE chain.

To simulate the interactions of the two polyelectrolytes, one 20-monomer PSS chain and one 10-monomer PDADMA chain were placed into a box with dimensions

of 10 nm x 5 nm x 5.7 nm. 10 Na-ions were added to make the net charge of the system zero. Figure 9 shows the initial configurations in water for single-PE and 2-PE systems. The original distance between the PE chains was 5 nm. These simulations will be later in the text referred to as the 2-PE simulations with initial configuration 1.

The 2-PE systems were built by cutting the polyelectrolyte, and ions and solvent in 1.5 nm radius from the PE from the final frame of the single-PE systems. Ions and solvent molecules were added to fill the 2-PE box, and to adjust the solvent composition and the number of ions to the desired level. This was done in order to improve the accuracy of the results, as the solvent shell was already equilibrated in the beginning of the simulations with the 2 PEs.

Because of the influence of the choice of the initial configuration on the obtained results, another set of 2-polyelectrolyte simulations were performed. PSS chain was rotated 90deg around the z-axis with respect to the initial configuration 1. These simulations will be later in the text referred to as the 2-PE simulations with initial configuration 2.

The use of small system size and periodic boundaries introduces systematic error to the results, and this error is referred to as finite size effects. In order to verify that the system size is big enough to produce relevant results, finite size effects have to be studied by comparing systems of different sizes. Finite size effects for the single-PE systems in water studied here were studied in[29]. Small variations were found between systems with PE chains of varying lengths[29]. However, these variations are not significant. Use of periodic molecules decreases finite size effects[29]. These results lead to the conclusion that the employed small system size unquestionably affect the results, but the effects do not compromise the relevance of the results.

5.3 Analysis methods

To assess the effect of solvent on the interactions of PSS and PDADMA in the simulated systems, various analysis methods were utilized. The employed analysis methods are presented in this section.

Previous chapters have demonstrated how polycations and polyanions interact in aqueous solution, and how the interactions might be affected by changes in the solvent quality and structure. Two phenomena that strongly affect the interaction properties of PEs are the counterion condensation and the hydration layer structure. The analysis methods thus concentrate on revealing these features from the studied systems. The particle positions, molecular orientations and hydrogen bonding are studied for the solvent molecules around the PEs.

Number density map presents the variation in the average number of chosen molecule or group per volume unit as colour gradient. The number densities are averaged over the trajectory. Number density map shows the density fluctuations and concentration gradients in the system. The number densities of solvent components were mapped around PSS and PDADMA to see the solvent shells and bulk solvent density fluctuations.

Radial distribution function

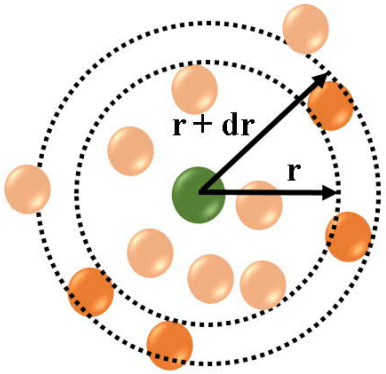

Figure 10: Radial distribution function gives the probability of encountering a particle between the distances r and $r + d$ from the reference particle.

$$RDF = \frac{\langle \rho_B \rangle}{\langle \rho_B \rangle_{local}} = \frac{1}{\langle \rho_B \rangle_{local}} \frac{1}{N_A} \sum_{i \in A}^{N_A} \sum_{j \in B}^{N_B} \frac{\delta(r_{ij} - r)}{4\pi r 2} \tag{23}$$

where $\langle \rho_B \rangle$ the density of particles B at a distance r from particle A, gives position correlations of two particle groups. The concept of radial distribution function (RDF) is presented in Fig. 10. RDF can provide useful information of the density of certain particles around a reference group. RDF can be calculated spherically, that is, in three dimensions around the reference particle. It can also be calculated in 2D, laterally, so that one axis direction is ignored. Cumulative radial distribution produces the average number of particles within distance r. Radial distribution functions were used in this thesis to evaluate intermolecular distances and distribution of solvent and ions around the polyelectrolyte.

To further analyse the behaviour of solvent in relation to the polyelectrolytes, hydrogen bonding between water and PSS was analysed. PDADMA does not form hydrogen bonds with water, and was not, therefore, analysed for hydrogen bonding. Gromacs tools were utilized to obtain hydrogen bond counts and lifetimes.

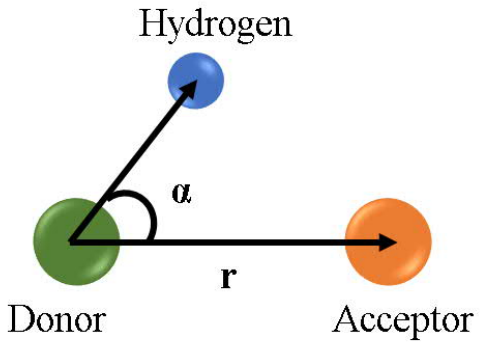

Figure 11: Hydrogen bond is defined by the angle between donor and acceptor, and the angle α.

To decide whether a donor and an acceptor are hydrogen bonded, geometrical criteria consisting of limits for the distance and angle between the hydrogen bond acceptor and donor were utilized. This geometrical definition for the hydrogen bonding is depicted in Fig. 11. The amount of bonds that met the criteria were calculated for each time frame, and a mean over the 200 ns trajectory was calculated to compare the average number of hydrogen bonds in different systems. The utilized values for the donor-acceptor distance r and angle α in this thesis were 0.27 nm and 30 deg, respectively. These were chosen to correspond to the first hydration layer around PSS.

Autocorrelation function gives the correlation of a time series with itself, delayed by time step τ. The autocorrelation function

$$C(\tau) = \langle s_i(t) s_i(t + \tau) \rangle \tag{24}$$

where $s_i(t)$ is the function for which the autocorrelation is calculated, and τ the delay between the two function values, is utilized to obtain temporal pattern information from time-series data. In this thesis, it was utilized to estimate hydrogen bond lifetimes, autocorrelation functions were calculated of the existence functions of the hydrogen bonds. The existence function is 1 if the bond exists at the given time, and 0 if it does not. To assess the hydrogen bond lifetimes, an average of all the autocorrelations of these existence functions was calculated.

Diffusion is the process where particles move from high concentration area to low concentration area as a result of random movement of the particles. Diffusion coefficient produces the relation of flux of particles to concentration gradient[108]. It can be obtained from the Einstein relation[108]

$$\lim_{t\to\infty}\langle \parallel \mathbf{r}_i(t) - \mathbf{r}_i(0) \parallel^2\rangle_{i\in A} = 6D_A t \tag{25}$$

where D_A is the diffusion coefficient, $r_i(t)$ and $r_i(0)$ the molecule positions at time t and 0, respectively. In this thesis, the diffusion coefficient was utilized when comparing the solvent component mobilities in the simulated systems. In addition to the hydrogen bond lifetimes, to further assess and analyse the mobility of the solvent molecules, the diffusion of the the solvent was studied.

6 Results and discussion

This section presents the obtained results on the effects of urea and ethanol on the interactions of PSS and PDADMA. The significance of these results is discussed, comparing them to relevant previous research on polyelectrolyte complexes, both experimental and computational. Analysis of the studied systems was performed to obtain information of the solvent effects on interactions of the PE complex. The results are discussed especially from the point of view of macroscopic polyelectrolyte materials, such as PSS-PDADMA multilayers, which are of interest e.g as functional coatings, as mentioned in previous chapters.

6.1 Simulation time and the model

As the results depend on the employed methods, the validity and limitation of the methods need to be assessed. This chapter presents and discusses results related to the validity of the model and choice of simulation duration.

Pure solvents were characterized for their physical properties in order to ensure basic validity of the modelled solvent systems before adding the polyelectrolyte to the system. The densities and density fluctuations were calculated for the solvent systems without polyelectrolyte. The temperatures and temperature fluctuations of the PE complex systems were calculated to check for appropriate system thermal behaviour in the presence of the PEs.

Binary mixtures of ethanol and water are known to separate at microscopic level[109,110]. Although urea and water mix quite well, some clustering of urea has been previously detected from MD simulations[111]. Solvent component clusters were observed in the simulations of this study in all binary systems, especially in those including ethanol. The relaxation time was chosen so that the densities of the solvent systems were equilibrated. The duration for the simulation production run was chosen so that the fluctuations in the solvent properties average over the simulation, and 200 ns was determined to be sufficient simulation time. To observe these averaged system properties, the results were calculated over the whole 200 ns simulation.

In order to ensure that the clusters and hydrogen bonding networks do not remain unchanged for the simulation, number density maps and system densities as a function of time were studied. The average densities of solvents were calculated from the solvent-only simulations to ensure that they agree with experimental data. These densities are presented in Table 1. The comparison of the densities from the simulations to the reference values shows that there are no great deviations. All of the errors in comparison to the experimental values are less than 2%. The error was calculated using block average method over five blocks using the full-precision average.

Table 1: Average solvent densities from solvent-only simulations at 300 K and literature reference values for the densities.

System	Simulated density (kg/m^3)	Reference value (kg/m^3)
Water	998 ± 0.001	997[112]
10 wt% Ethanol	976 ± 0.017	982[113]
30 wt% Ethanol	943 ± 0.002	942[113]
10 wt% Urea	1027 ± 0.094	1027[114]
30 wt% Urea	1098 ± 0.013	1079[114]

In addition to the densities, the temperatures and temperature fluctuations were calculated in order to assess the accuracy of the model. These were calculated for 2-PE systems, to assess the effect of thermostatting groups. As mentioned in chapter 5, the systems were divided to two groups with their own thermostats. Because artefacts may arise form an incorrect choice of the thermostatting groups[115], the choice of these groups is shortly assessed. Table 2 contains the average temperatures and standard deviations of the two thermostatting groups in the 2-polyelectrolyte systems.

Table 2: Average temperatures and standard deviations (SD) for thermal coupling groups in 2-polyelectrolyte systems. Group 1 consists of water and ions, Group 2 of polyelectrolytes and ethanol/urea.

System	T (K), Group 1	SD (K)	T (K), Group 2	SD (K)
Water	300	2.3	299	15.7
10 wt% Ethanol	300	2.5	300	4.9
30 wt% Ethanol	300	2.2	300	2.9
10 wt% Urea	300	2.4	300	5.4
30 wt% Urea	300	2.6	300	3.3

The results in Table 2 show that the average temperatures do not differ significantly, and that the average temperatures are at the reference temperature of 300 K. However, the fluctuation is significantly higher in the water system, as the second thermocoupling group solely consists of the PEs. When the concentration of the additive increases, the number of atoms in the second thermocoupling group increases, and the temperature fluctuations decrease.

There is no ideal way to divide the system to thermocoupling groups. The results should be interpreted taking into consideration the possible faults of the model, such as the momentary differences in the temperature/kinetic energy of the different parts of the system. Nevertheless, as demonstrated above, the densities of the solvents do not deviate very significantly from the literature values, and the total density fluctuates very little.

The ability of the model to reproduce the solvent densities, and the desired average temperature with relatively small fluctuations indicate that the model is

good. Although the validity of all the results obtained from the simulations cannot be decided using these measures, the result presented in this chapter indicate that the model can reproduce phenomena related to water-based solutions. The results presented in this chapter do not disprove the validity of the model.

6.2 Polyelectrolyte pairing

This chapter presents results and discusses the binding of the PEs in the studied systems.

6.2.1 Ethanol

In all systems where both PSS and PDADMA are present, they form a complex, i.e. the oppositely charged groups of the PEs associate, and the structure remains paired for the rest of the simulation. Like in Figure 12, which is a snapshot of the associated PE structure from the 10wt% urea system, in all systems both extrinsic and intrinsic pairing occurs, i.e. the PSS charge groups bind to both sodium ions and PDADMA monomers.

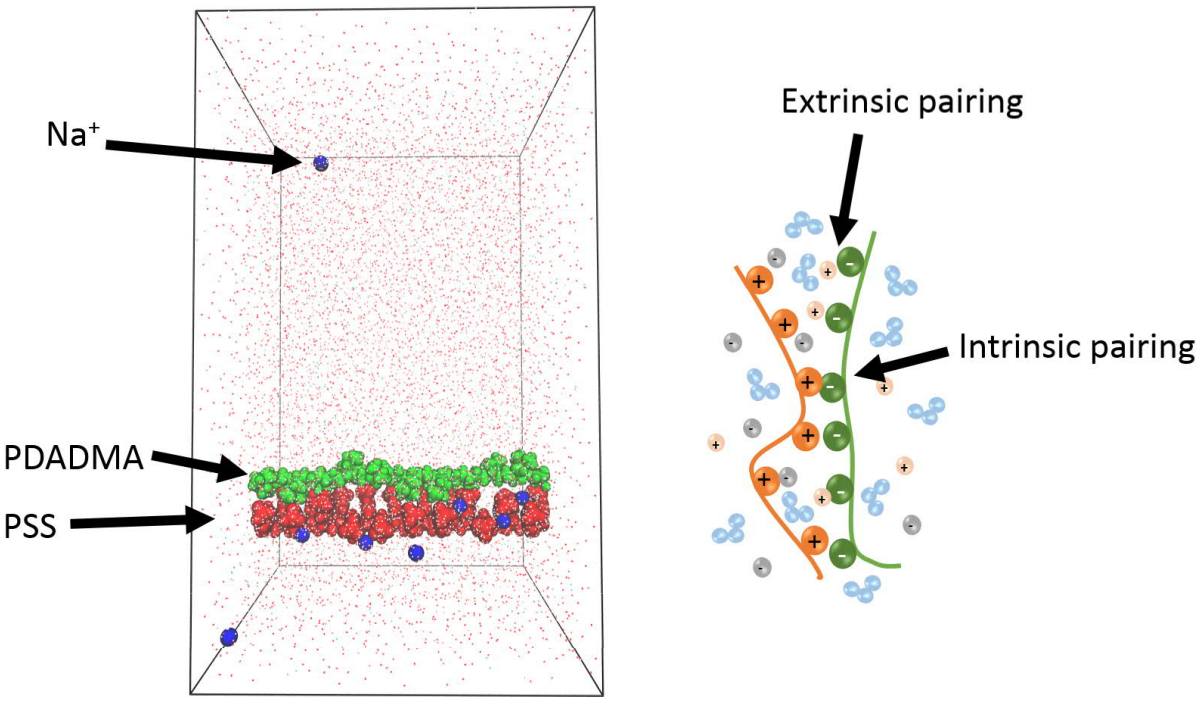

Figure 12: PSS-PDADMA complex with Na-ions in 10 wt% ethanol shows both extrinsic and intrinsic pairing.

The characteristics of the complex, such as the distance between the polyelectrolytes and the magnitude of counterion condensation vary from system to system, due to the effect of ethanol and urea. The pairing of the PEs was studied using

radial distribution function calculated between the backbone atoms of PSS and PDADMA to estimate the effects of the additives on the PE pairing. These results are presented in Fig. 13. The backbone distances can be approximated from peaks of the radial distribution function, as the probability of the PEs being at the distance range indicated by the peak is the highest. The relative peak positions can provide information on the differences in the PSS-PDADMA distances, and, consequently, on the effects of the additives on the PE separation.

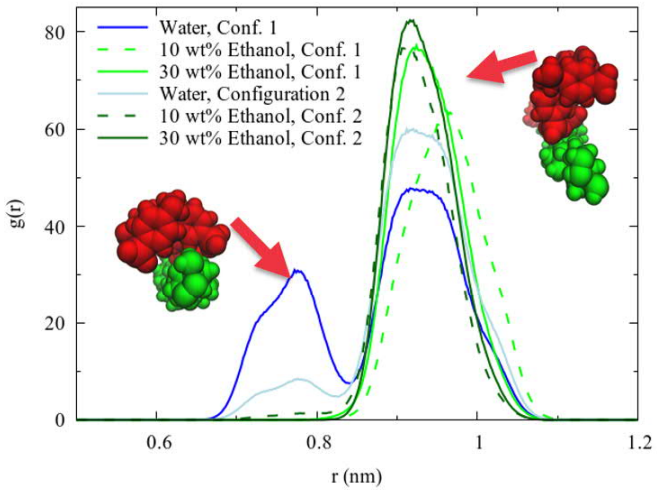

Figure 13: 2D-radial distribution function g(r) between the backbone atoms of PSS and PDADMA. The peaks indicate the distances of PSS and PDADMA in different solvents. The peaks at 0.75 nm and 0.9-1 nm correspond to two different side chain conformations (see inset). The two datasets correspond to the two initial configurations.

All systems show a peak in the PSS-PDADMA backbone RDF at 0.9-1 nm. In addition to this peak, another, lower-intensity peak at 0.8 nm is present for the pure water systems and the 10 wt% ethanol system with the initial configuration 2. The two peaks present are caused by two different complex binding conformations, pictured in Fig. 13. In the conformation that is present in all of the 2-PE-systems, half of the PSS charge groups are pointed towards the charges in the PDADMA chain, and half away from the PDADMA chain, to the solution. In the close binding conformation, however, all of the PSS charges point towards the PDADMA charges. This way the backbones of the two PEs come closer, as PDADMA is between the PSS sidechain. With both initial configurations, the pure water systems show wider distance distributions. This could indicate that the chains can move more freely in pure water than in the presence of ethanol. This will be further discussed in following chapters.

Although there are differences between the results from the two setups, the closer complex binding conformation seems to occur when sufficient amount of water is

present. The reasons for this effect are not evident from the results. One possible explanation is the ability of the hydrocarbon backbones of the PEs to interact via hydrophobic interactions. These interactions are supposedly more pronounced with higher water content, as the interactions of solvent and PE backbones are less favourable than in the presence of ethanol, and could thus lead to this closer-binding conformation.

In the presence of ethanol the complex is (mostly) in the extended side chain conformation. The increasing amount of ethanol gives different results for the two initial configurations. The 30 wt% ethanol system shows decreased backbone distance in comparison to the 10 wt% ethanol system in the initial configuration 1. The 10 wt% system with initial configuration 1 shows increased PSS-PDADMA distance compared to the pure water system with the same initial configuration. The configuration 2 systems show similar PSS-PDADMA distances for both of the ethanol systems. Thus, clear trend is not distinguishable for the effect of ethanol on the PSS-PDADMA distance. Nevertheless, it is possible that addition of certain amount of ethanol could increase the PSS-PDADMA backbone distance. Ethanol decreases the polarity of the solvent, and thus changes the solvent quality for the PEs.

The molecular dynamics simulations of single PEs, including PSS, in different solvents by Smiatek et al.[116] indicate that the radius of gyration of the PE is largest in solvent of intermediate polarity, rather than in water. Smiatek et al. account this effect for the balance of hydrophobic and hydrophilic interactions resulting from the chemical character of the PEs. Smiatek et al. used different force field, but obtained similar results from similar systems. These results support the effect of the addition of ethanol on the PE-backbone distance here observed for the initial configuration 1.

Radius of gyration can be utilized as a measure of the solvent quality, as described in Section 2.1.2. When considering polyelectrolyte complexes and assemblies, decreasing solvent quality decreases the solvent uptake of the PE assembly[70]. Thus, one possible explanation for the effect of ethanol for the backbone distance observed in the configuration 1 systems is that the small addition of ethanol in fact improves the solvent quality in comparison to water, whereas in the 30 wt% the PEs come closer together due to the decreased electrostatic screening. However, as mentioned above, the trend is not similar for the configuration 2 systems, and the data is not conclusive for the effect of ethanol on the PSS-PDADMA distance.

The results of classical MD simulations depend on the initial configuration, because in finite-length simulations it is not possible to sample all possible configurations of the system. Thus, with this dataset it is not possible to confirm whether or not this close-binding conformation could occur in the other systems as well. Comparing the results from the simulations with different initial configurations confirms the fact that the results of this research depend on the initial configuration. However, both datasets studied here give very similar results for systems other than the 10 wt% ethanol systems in the backbone-backbone RDF above. This indicates, as well as the fact that the methods employed here are widely utilized and recognized, that the results of this thesis can still be considered meaningful. However, thorough verifying of the observed effects would require the study of additional datasets.

To further study the reasons and mechanisms that affect the interactions between

PSS and PDADMA, the distribution of the solvent molecules were studied using solvent density mapping. The number density map presents the number of chosen solvent component in the xy-plane of the box as a colour gradient from 0 to the maximum number density of the component.

Ethanol number density maps (Fig. 14) show ethanol distribution around the PSS-PDADMA complex. The figures reveal strongly asymmetric condensation of ethanol around the PE complex in the 30 wt% ethanol solvent. At the lower ethanol concentration the condensation does not seem to be as asymmetrical. However, from the simulation trajectories it is evident that the PEs move more in the 10 wt% ethanol than at the higher concentration. Thus, in the density map the positions of the PEs are not fixed, and although the condensation would occur at certain site of the complex, it would not be visible in the solvent number density map, which is averaged over the 200 ns simulation trajectory.

Ethanol is present between the PEs, but at smaller density than in the bulk solvent. The interaction between the PE charge groups and the low-polarity ethanol is not energetically favourable, and as the charged parts of the PEs point mainly towards each other, in other words, to the centre of the complex, ethanol mostly remains outside the complex. This agrees with experimental results, as PSS/PDADMA multilayers have been experimentally observed to have a small ethanol uptake[70].

To summarize, the number density figures suggest that the condensation of ethanol occurs around the complex, as the number density is higher there than in the bulk solvent. Ethanol could cause a decrease in the dielectric constant of the solvent, and this effect could be locally more pronounced at the PSS backbone than in the bulk solvent. However, the obtained results indicate that this phenomenon has no effect on the PSS-PDADMA distance. The asymmetrical condensation of ethanol at the complex arises from the differences in the condensation around PSS and PDADMA. These differences are demonstrated in Figure 15, which shows ethanol number densities in single-PE-systems.

The ethanol number density maps for the single-PE systems demonstrate that ethanol condenses around PSS, but not around PDADMA. From simulation snapshot (Figure 16) it can be confirmed that the strongest condensation occurs at the backbone of the PSS. The condensation results from hydrophobic interactions between the hydrocarbonous backbone of PSS and ethanol. The charges in PSS are more localized and further away from the apolar backbone than in PDADMA, where the charge is a part of a ring structure, and thus more delocalized. Therefore, condensation does not occur at PDADMA, but instead a depletion area is observed around the PE. The repulsive electrostatic forces in this system are stronger than the attractive hydrophobic ones and thus ethanol is repelled by the polar, charged groups of PSS and PDADMA.

The previously described condensation of ethanol could have an effect on the distribution of water, and consequently, the interactions of the two PEs. Thus, number density mapping was also used to assess water distribution around the PE complex in the presence of ethanol (Fig. 18 and 19).

In addition to the ethanol condensation around PSS, ethanol depletion is observed outside the condensation shell. This probably results from water condensation layer

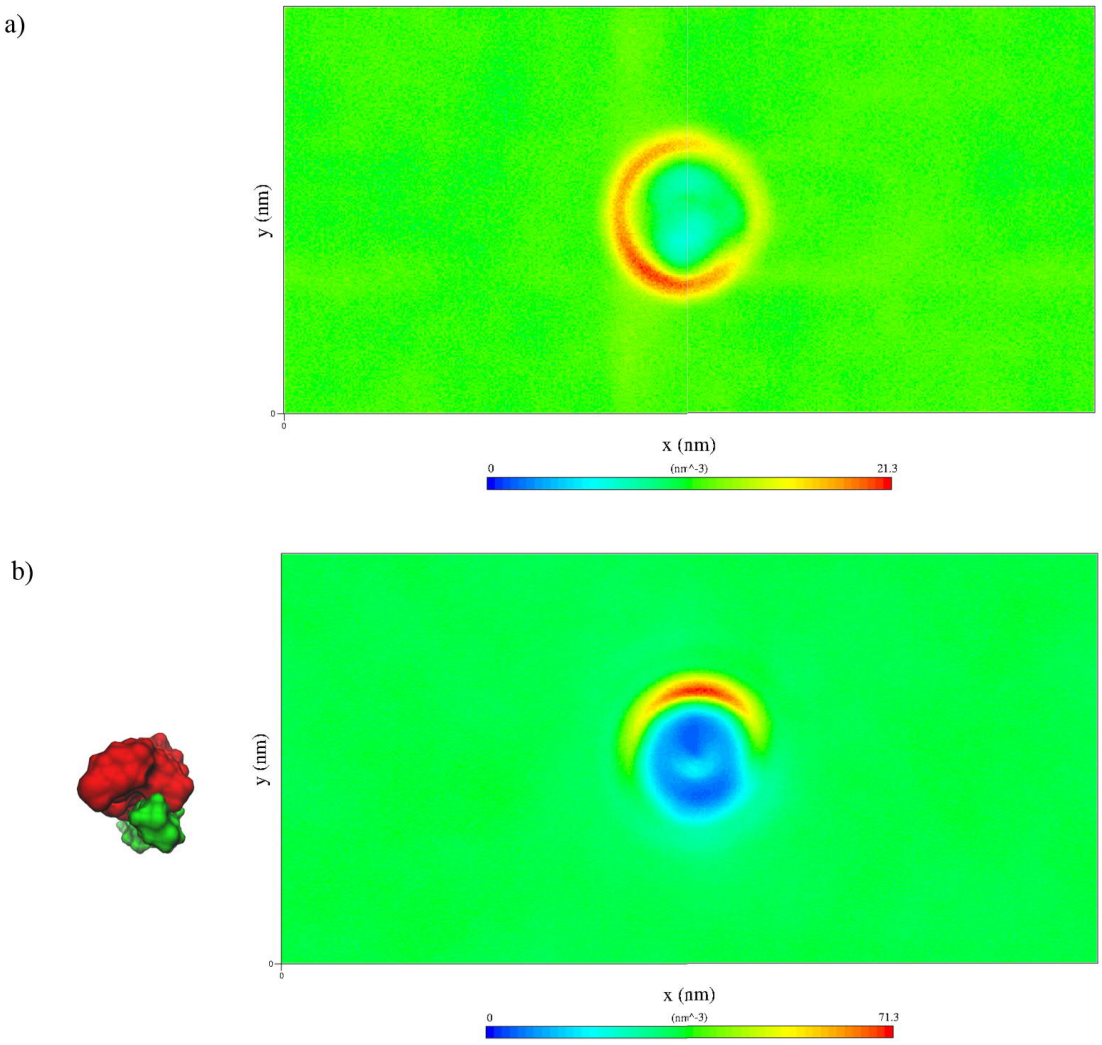

Figure 14: Ethanol number density around PSS-PDADMA-complex in a) 10 wt% ethanol b) 30 wt% ethanol. On the left are the positions of the two PEs in the number density map in 30 wt% ethanol, PSS in red and PDADMA in green (not presented for 10 wt% due to changes in the relative positions of the two PEs). Ethanol shows condensation around the PE-complex. In 30 wt % ethanol the condensation is strongly asymmetrical. PSS-PDADMA complex is perpendicular to the plane.

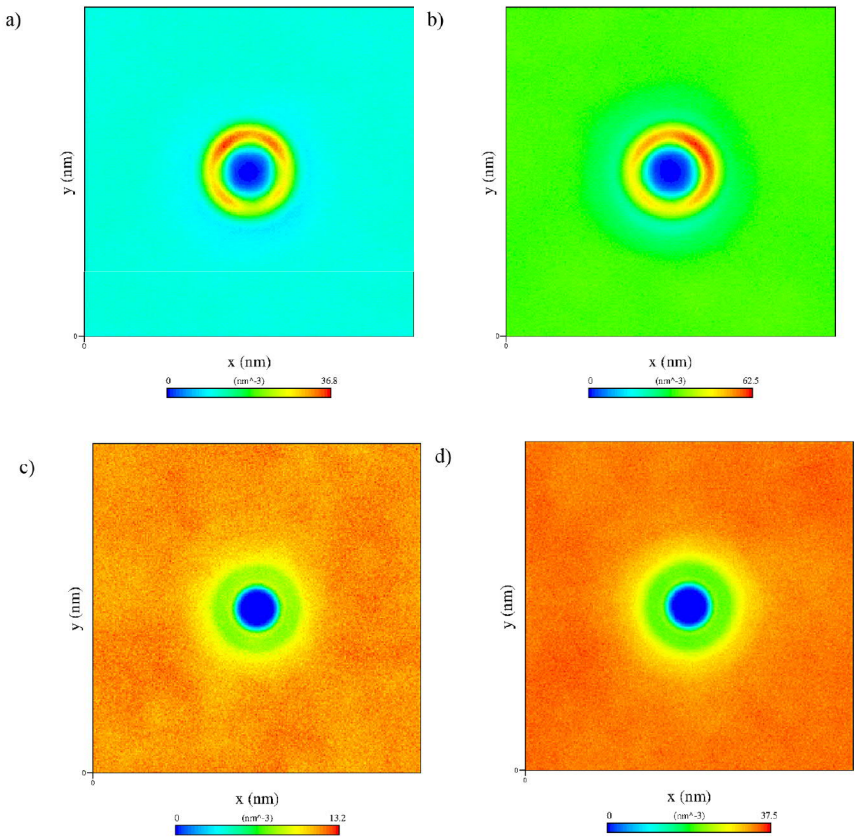

Figure 15: Ethanol number density around a) PSS in 10 wt% ethanol b) PSS in 30 wt% ethanol c) PDADMA in 10 wt% ethanol and d) PDADMA in 30 wt% ethanol. Strong condensation is observed around PSS, whereas around PDADMA there is depletion of ethanol. Polyelectrolyte axis is perpendicular to the plane.

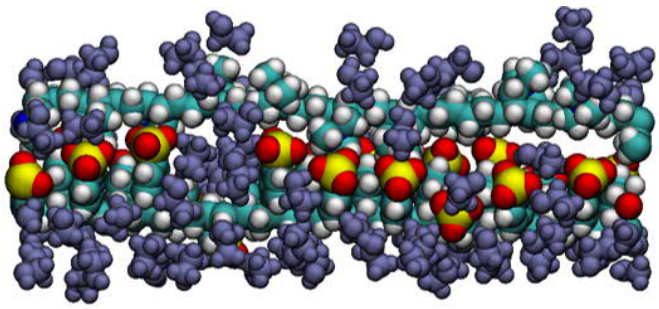

Figure 16: Snapshot of the PSS-PDADMA complex in 30 wt% ethanol, PDADMA above and PSS below it. Ethanol molecules in purple, water and ions omitted to visualize the distribution of ethanol around the complex. Ethanol condenses strongly to the backbone of the PSS chain.

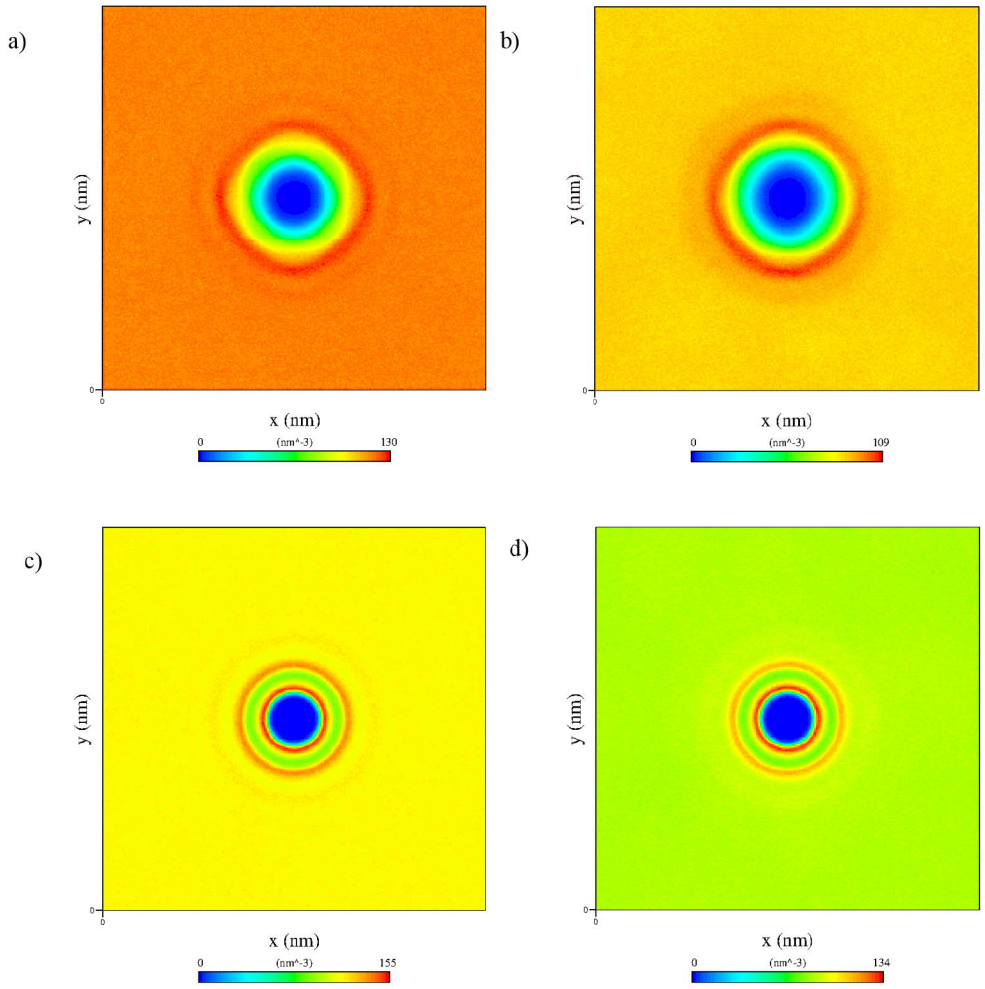

Figure 17: Water number density around a) PSS in 10 wt% ethanol b) PSS in 30 wt% ethanol c) PDADMA in 10 wt% ethanol and d) PDADMA in 30 wt% ethanol. Water condensation and depletion rings are seen in all systems around the polyelectrolytes. Polyelectrolyte axis is perpendicular to the plane.

at that area, which can be seen from single-PE-system water number density maps in Fig. 17.

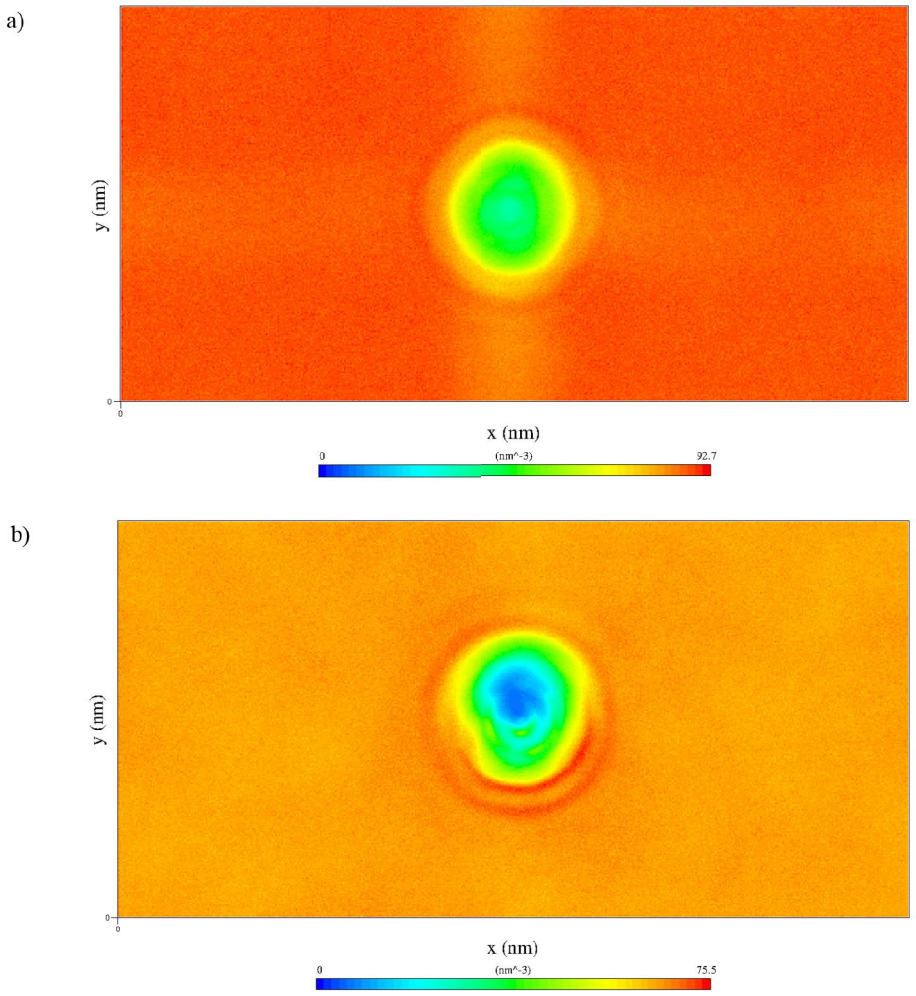

Figure 18: Water number density around PSS-PDADMA-complex in a) 10 wt% ethanol b) 30 wt% ethanol. Polyelectrolyte complex is perpendicular to the plane.

Around PDADMA both water condensation and depletion rings are visible in ethanol systems. One depletion ring is also visible in pure water systems, both in single-PE (Fig. 19) and PSS-PDADMA systems (Fig. 18).

The water number density maps for 2-PE ethanol systems (Fig. 18) show at least one water condensation ring in both ethanol systems around the complex. In addition to this, the 30 wt% ethanol system shows second condensation ring near the area were PDADMA is mostly located. The 2-PE pure water system (Fig. 20) shows two depletion rings, but no condensation rings.

In single-PE systems PDADMA shows a higher number of solvent shells than PSS. This could be a result of the charge of PDADMA being more delocalized than that of PSS. The charge is thus more evenly distributed on the PE chain, and orientation

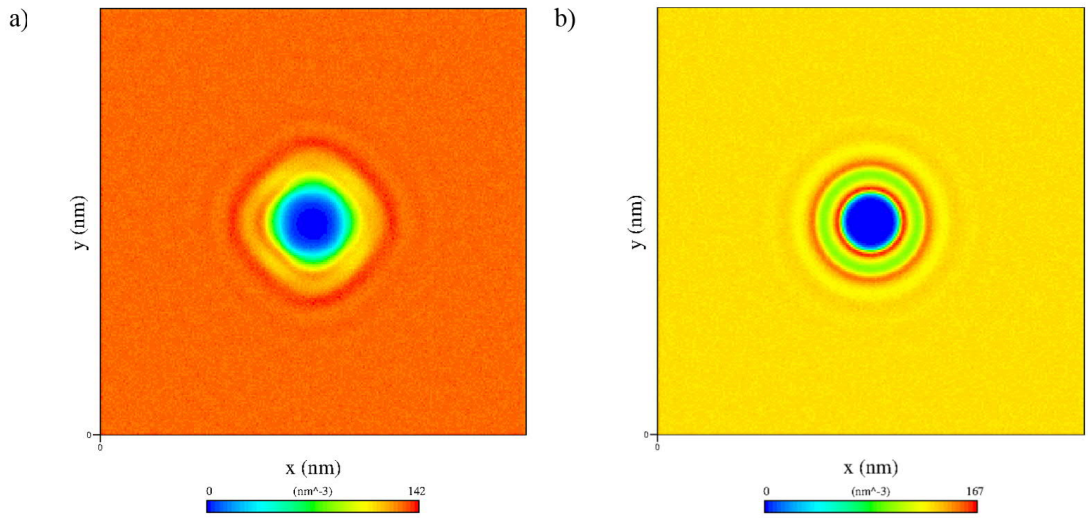

Figure 19: Water number density around a) PSS b) PDADMA in single- polyelectrolyte systems in 100 % water. Polyelectrolyte axis is perpendicular to the plane.

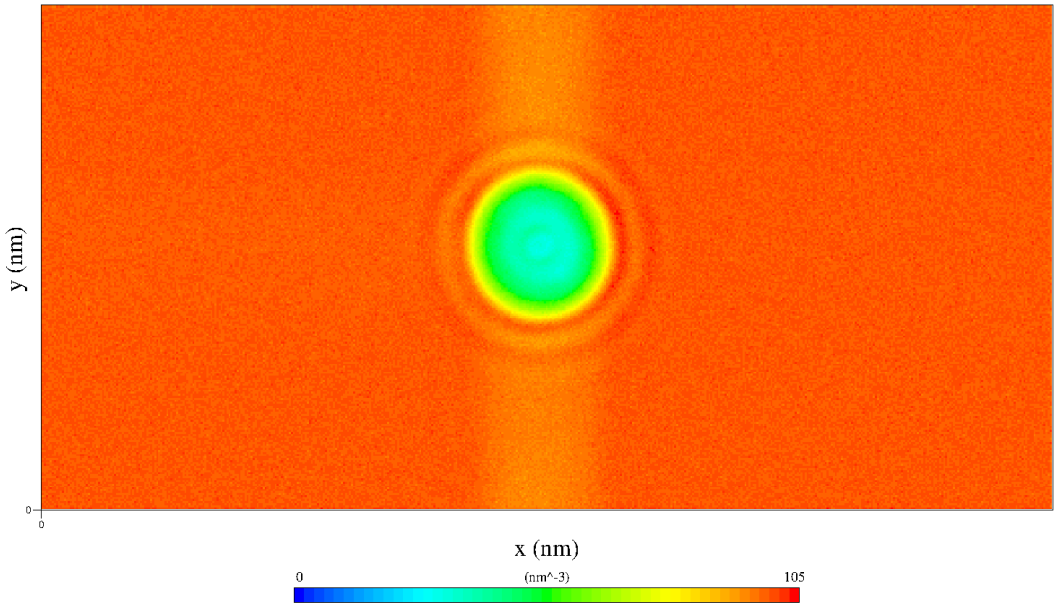

Figure 20: Water number density around PSS-PDADMA-complex in water. Polyelectrolyte axis is perpendicular to the plane.

of water dipoles is affected all around PDADMA. The sulfonate groups of PSS move, thus the charges move, and the PSS-solvent interactions change, presumably more than PDADMA-solvent interactions, resulting in differences between the solvation shells of the two PEs.

To summarize, it was observed that the number and structure of the solvent shells around PSS and PDADMA are altered by the addition of ethanol. The changes in the solvation shell can change the electrostatic screening and chemical environment around the PE. These factors in turn alter the interaction with other molecules, such as other PEs and counterions. The condensation effects of ethanol consist of the condensation around PSS, depletion around PDADMA and around the complex at ethanol concentration of 30 wt% these effects combine to produce a very asymmetrical condensation, which is located at the PSS backbone. The solvent quality change caused by ethanol is not straightforward to interpret, as the chain coil packing cannot be used as a measure, and the results on the effect of ethanol on the PE separation are unclear. Ethanol decreases the solvent dielectric constant, and presumably the solvent conditions become poorer with the addition of ethanol, at least when the ethanol concentration is high enough. When the solvent conditions are poorer for the charged species, they tend to come closer together. Although the effects on the separation of PSS and PDADMA cannot be established with these results, counterion condensation could be increased by the decreased dielectric constant of the solvent caused by the addition of ethanol. The observed condensation of ethanol brings ethanol molecules closer to the PSS, where the sodium ions can compensate the PE charges. Counterion condensation can change the effective charge of the polyelectrolyte, and therefore affect the PE complex.

6.2.2 Urea

As described in the Section 5, the effect of urea on the polyelectrolyte interactions were studied at two different urea concentrations, 10 wt% and 30 wt%. Urea is polar, and it disturbs water hydrogen bonds by forming its own hydrogen bond network and thus changes the behaviour of the solvent. The behaviour of solvent was studied for the urea systems similarly as for the ethanol systems, in order to study how urea increases the PSS-PDADMA backbone distance.

The radial distribution functions were calculated between the backbone carbon atoms of PSS and PDADMA to assess the effect of addition of urea on the PE interactions. Like the ethanol systems, all urea systems show a peak in the PSS-PDADMA backbone carbon RDF at 0.9-1 nm. The shifts in these peaks in Figure 21 show that the backbone distance increases with increasing urea concentration. This effect is more pronounced for the systems with initial configuration 1, but still distinguishable for the other two systems as well. As urea does not decrease the polarity of the solvent, and thus presumably does not decrease the solvent quality, at least to the same extent that the 30 wt% ethanol does, urea does not push the charged species together. Urea presumably interacts with the PE charge groups via e.g. hydrogen bonding, and therefore pushes the PEs apart.

The urea number density maps from the 2-polyelectrolyte systems (Fig. 22) show

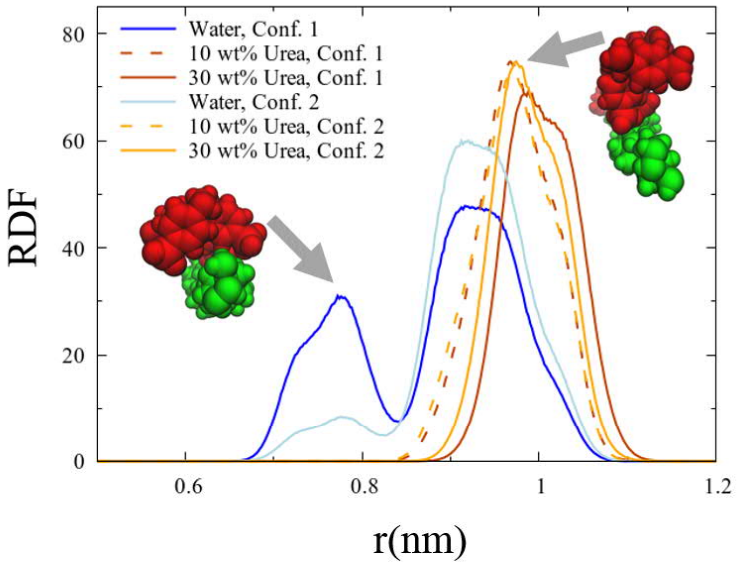

Figure 21: 2D-radial distribution function between the backbone atoms of PSS and PDADMA. Peaks give the backbone distances between the PEs. The peaks at 0.75 nm and 0.9-1 nm correspond to two different side chain conformations (see inset). Conf. 2 refers to the second initial configuration.

condensation of urea around the complex. The urea number density between PSS and PDADMA is higher than in the bulk solvent, which demonstrates that urea goes between PSS and PDADMA. Being a polar molecule, it can interact with the charged areas of the polyelectrolytes.

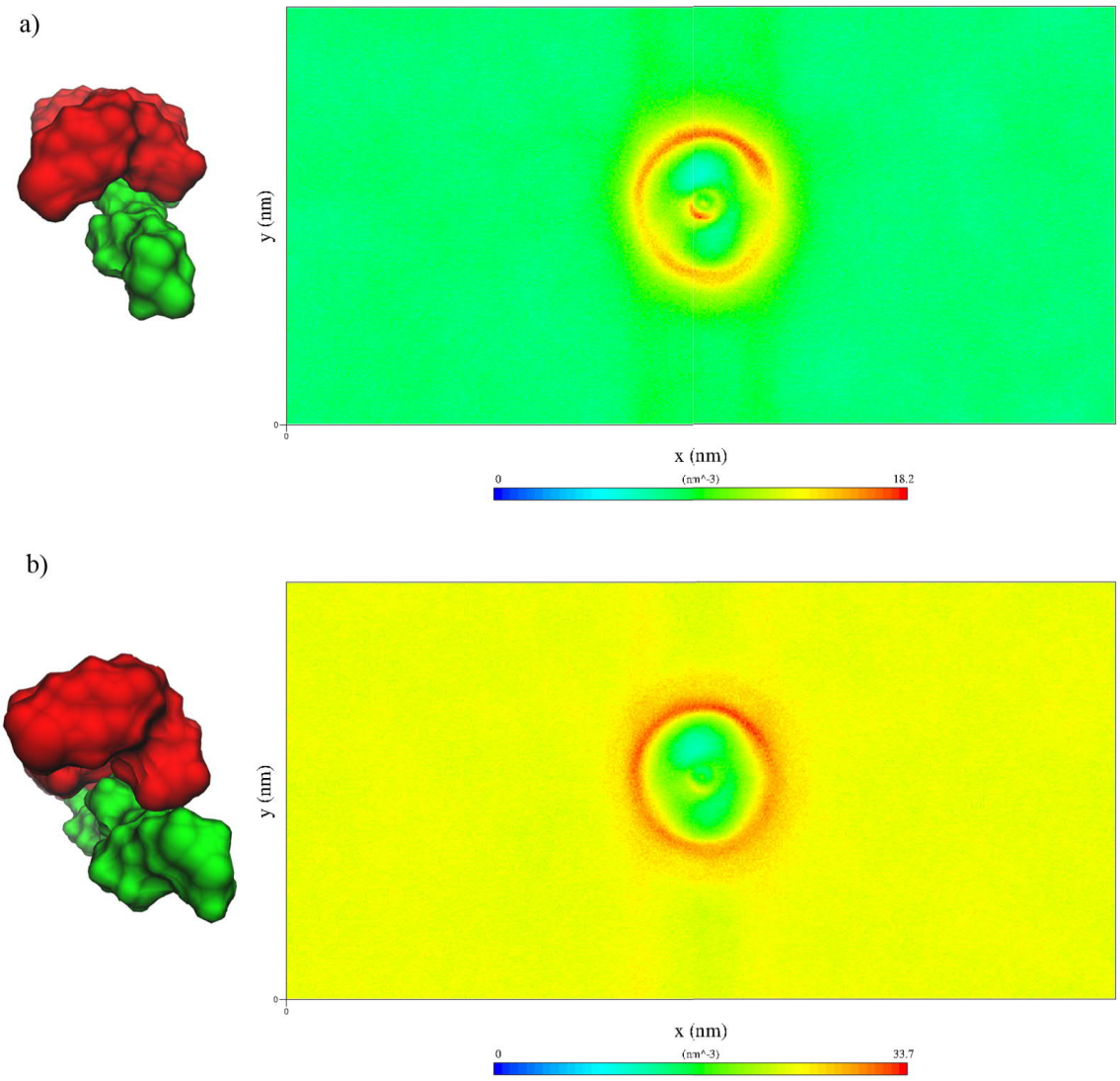

Figure 22: Urea number density around PSS-PDADMA-complex in a) 10 wt% urea b) 30 wt% urea. Corresponding approximative relative positions of PSS and PDADMA on the left, PSS is red and PDADMA green. Condensation of urea is observed around the complex, as well as between the PEs, as higher number density compared to the surrounding solvent. Polyelectrolyte complex is perpendicular to the plane.

In the single-PE systems the number density graphs (Fig. 23) demonstrate condensation of urea around both PEs, especially strongly at the higher urea concen-

tration. The density degrades quite smoothly, and no clear condensation or depletion rings are observed. Thus, as a consequence of this condensation behaviour around single PEs, when the two PEs are in the same solution, urea condenses around the complex, and around both individual PEs, i.e. penetrates the complex and pushes PSS and PDADMA apart.

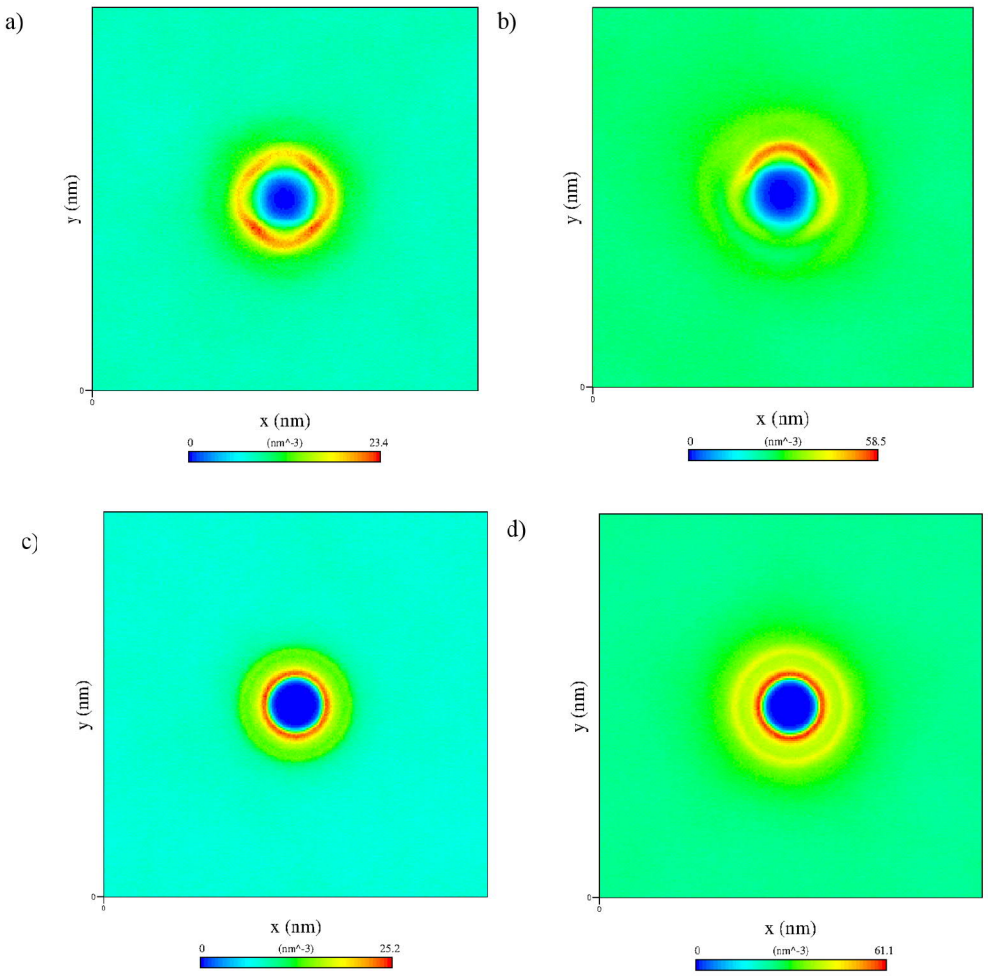

Figure 23: Urea number density around a)PSS in 10 wt% urea b)PSS in 30 wt% urea c)PDADMA in 10 wt% urea and d)PDADMA in 30 wt% urea. Urea condensates strongly around both polyelectrolytes.

The water number densities plotted in Figures 24 and 25 in the presence of urea for single-PE-systems and PE-complex systems, respectively, show both condensation and depletion shells around the individual PEs and the complex. Especially a larger depletion is observed in the vicinity of the macromolecules compared to the pure water systems. Because urea condenses at the PEs, water goes further away from the PE.

Urea clearly causes the polycation-polyanion distance to grow, presumably because

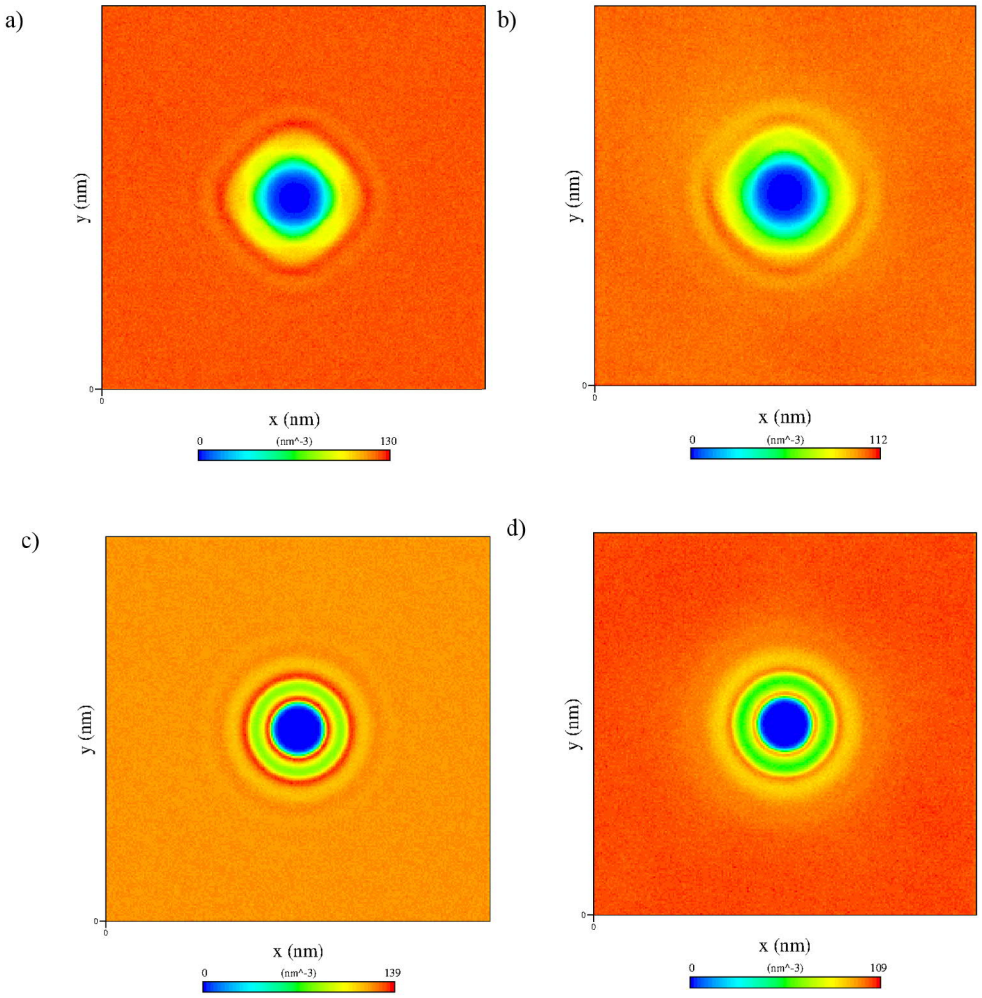

Figure 24: Water number density around a)PSS in 10 wt% urea b)PSS in 30 wt% urea c)PDADMA in 10 wt% urea and d)PDADMA in 30 wt% urea. Multiple solvation shells are visible in the density maps.

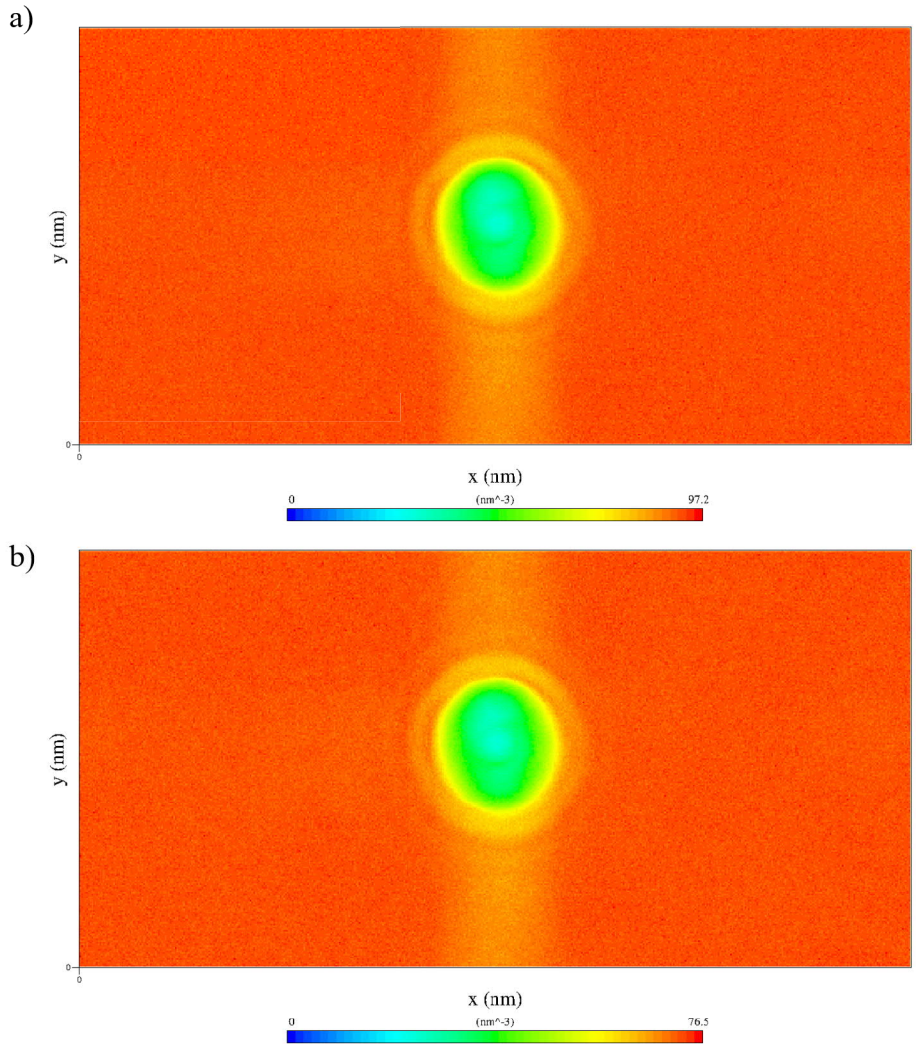

Figure 25: Water number density around PSS-PDADMA-complex in a) 10 wt% urea b) 30 wt% urea. Multiple solvation shells are visible in the density maps.

it is attracted by the PE charges, penetrates the complex and hydrogen bonds with PSS sulfonate groups. In larger systems, such as PE assemblies, urea could affect quite significantly the properties of the assembly, such as mechanical and thermal properties. Stiffness of the assembly might decrease, as the PSS-PDADMA distance is larger and the PEs could therefore be more loosely bound, decreasing the viscosity of the material. Thermal softening occurs when water and PE chains become more mobile due to increased kinetic energy of the particles (increased temperature). The results indicate that urea would affect the mobility of the chains in the system, and thus it could affect the thermal softening of PE assemblies. This will be discussed further in following chapters.

6.3 Hydrogen bonding

The previous sections demonstrated that addition of ethanol or urea changes the water distribution around the individual PEs and the PSS-PDADMA complex. PSS and water interact via hydrogen bonding, so analysing the hydrogen bonds both in water and in the presence of ethanol and urea provides useful information of the PE-water interactions. The number density maps showed that both ethanol and urea can stay between the PEs, although urea is more abundant inside the complex than ethanol. Thus their effect on the PE-water interactions must be estimated, as these interactions are crucial for the properties of the polymer complex.

Water-PSS hydrogen bonds were analysed in terms of number and lifetime. The cut-off 0.27 nm for the hydrogen bonding was chosen by looking at the first peak in the rdf between PSS charge groups and water (Fig. 26) in the 2-PE-systems. The cut-off corresponds to the minimum after the first peak, as the group of water molecules closest to the PSS charge groups can be assumed to be hydrogen bonded. Geometrical criteria (angle 30 deg and donor-acceptor distance 0.27 nm) were utilized, because they have proven superior in comparison to energetic hydrogen bond criteria[117].

In addition to the peak already mentioned, three other peaks can be distinguished from the water-PSS rdf. All of the peaks correspond to solvation shells. The first solvation shell is hydrogen bonded to PSS, whereas the next solvation shells are bonded to each other. The PE determines the orientation of the first solvation shell.

The number of PSS-hydrogen bonds (Table 3) show that the number of PSS-water hydrogen bonds decreases with increasing ethanol concentration. With the addition of ethanol and its condensation at PSS backbone, the amount of water molecules near the sulfonate groups of PSS decreases significantly. Also, as mentioned previously, dehydration of PEMs have been observed in the presence of organic solvents[16].

Highest number of PSS-water hydrogen bonds is observed in the pure water system. Decreasing amount of water results in decreasing PSS-water hydrogen bond number. Urea results in larger decrease of hydrogen bonding than ethanol. None of the systems show 100 % of the theoretically possible hydrogen bonds between water and PSS. In addition to the solvent, the PSS sulfonate groups interact with counterions and PDADMA charges, which presumably decreases the hydrogen bonding. Urea penetrates inside the complex, which probably decreases the amount of water between the PEs. From the number density maps presented in previous

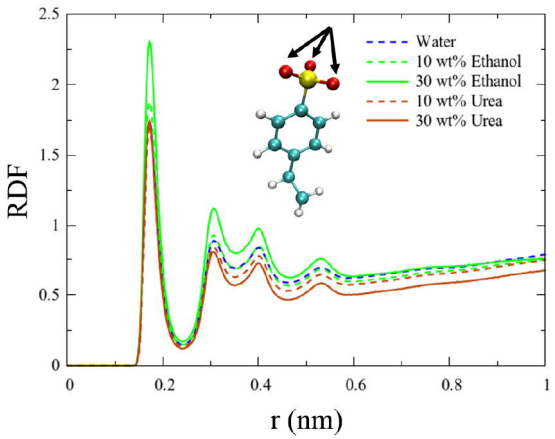

Figure 26: 2D-radial distribution functions between water hydrogens and PSS sulfonate oxygens in the 2-PE-systems. Peaks imply the positions of hydration shells.

Table 3: Number of PSS-water hydrogen bonds in 2-PE systems, averaged over last 200ns of the trajectory, and error estimate for this average. Error estimate is based on the standard error of mean, i.e. standard deviation divided by the sample size. Last column presents the percentage of hydrogen bonds formed per possible hydrogen bonding site.

System	Number of hydrogen bonds	% of possible hydrogen bonds
Water	44.81 ± 0.02	0.75
10 wt% Ethanol	42.97 ± 0.03	72
30 wt% Ethanol	39.30 ± 0.02	66
10 wt% Urea	40.90 ± 0.02	68
30 wt% Urea	35.20 ± 0.02	59

sections it was observed that ethanol is also present between PSS and PDADMA, but not in as large amounts as urea. Thus, the hydrogen bonding data is consistent with the previously presented results.

In addition to the amount of the number of the PSS-water hydrogen bonds, their lifetime was calculated using autocorrelation functions, see Eq 24. The results for the two-PE systems are presented in Figure 27.

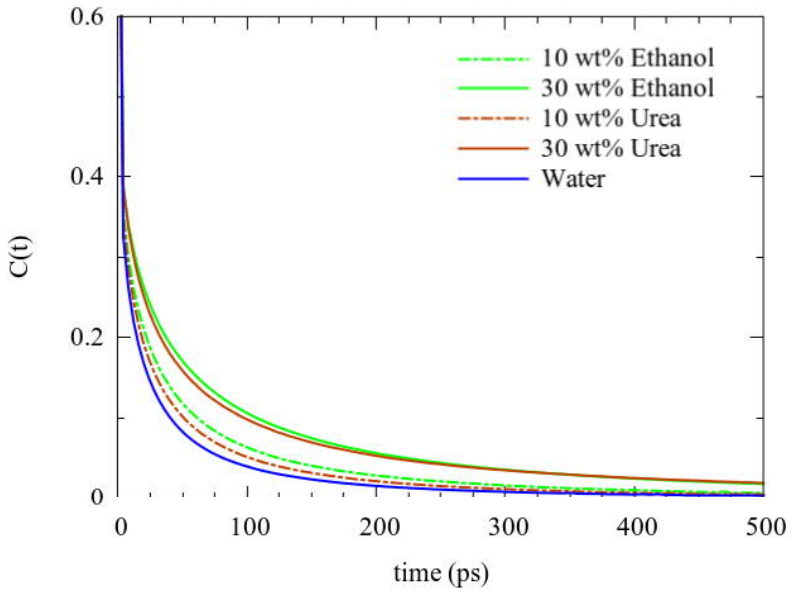

Figure 27: PSS-water hydrogen bond autocorrelation functions C(t) for 2-PE-systems. Calculated as the average of the correlations of the existence functions for the hydrogen bonds.

The autocorrelation function is the average of the autocorrelations of all the PSS-water hydrogen bonds in the system. The value of the autocorrelation for the given hydrogen bond is 1 if the hydrogen bond exists, and 0, if it does not exist anymore. When the average reaches zero, all of the hydrogen bonds present at time 0 have been broken. The maximum lifetime of the hydrogen bonds is the time where the average autocorrelation reaches zero.

The hydrogen bond lifetime analysis via the autocorrelation shows that for the studied systems, the less water there is in the system, the longer the PSS-water hydrogen bond lifetime is. The addition of ethanol results in a larger increase in the hydrogen bond lifetime than the addition of urea. The complex could thus be more stable in the presence of urea and ethanol than in pure water, as the mobility of the water in the vicinity of the PSS-PDADMA complex is reduce. The number of PSS-water hydrogen bonds is reduced in the presence of additives, which might mean dehydration of the complex. Water acts as a plasticizer, so dehydration decreases chain movement. These indicators of mobility decrease are in line with the wider PE-PE distance distribution observed for pure water systems, which indicated that the PE chains could be more mobile in pure water than in the presence of ethanol or urea.

6.4 Solvent diffusion

The PSS-water hydrogen bond lifetimes presented and discussed in previous section indicate that the addition of ethanol could slow down the solvent. Solvent diffusion coefficients (Table 4) were calculated for both water and ethanol to verify the effect. The results show significant reduction of the diffusion rate with increasing ethanol concentration: 22% reduction from water to 10 wt% ethanol, 33% reduction from 10 wt% ethanol to 30 wt% ethanol, which corresponds to 47% reduction compared to water. The same trend is observed for urea: 10 wt% urea shows 5% reduction in water diffusion coefficient from pure water system and 30 wt% urea 21% reduction from water.

Table 4: Diffusion coefficients for solvent components in the PSS-PDADMA-systems show decrease in diffusion rate with decreasing system water content. D_W and $D_{Additive}$ are the diffusion coefficients for water and ethanol/urea, respectively.

System	$D_w(1\text{x}10^{-5}\text{cm}^2/\text{s})$	$D_{Additive}(1\text{x}10^{-5}\text{cm}^2/\text{s})$
Water	3.71 ± 0.10	
10 wt% Ethanol	2.90 ± 0.03	1.68 ± 0.04
30 wt% Ethanol	1.95 ± 0.05	1.17 ± 0.03
10 wt% Urea	3.51 ± 0.02	1.82 ± 0.0002
30 wt% Urea	2.94 ± 0.02	1.50 ± 0.11

Compared to the pure water system, all other systems show smaller diffusion coefficients. For ethanol, the decrease in the coefficient is larger than for urea. For both urea and ethanol systems, the 30 wt% systems have smaller diffusion coefficients than the 10 wt% systems. The trends are similar to the additive diffusions. The diffusion coefficients for urea and ethanol are significantly smaller than those of water in the same systems.

Smaller diffusion coefficients indicate slower solvent diffusion, which results in increased PE complex stability, as the chains are less mobile[60]. The decreased water mobility could also result in higher thermal transition temperatures for PE assemblies, which has already been indicated by experiments for PSS/PDADMA PEMs in the presence of ethanol[70]. Urea both increases the PE-PE-distance and restricts the chain mobility, and could thus make PE assemblies softer, but more stable than those in pure water.

Miller et al[70] have studied experimentally PEMs in ethanol and water at low NaCl concentrations. Their results[70] indicate that ethanol decreases swelling. This is consistent with our results, as the PSS-PDADMA backbone distance gets smaller with increasing ethanol concentration. However, the PSS-PDADMA distance is smaller in water than in 10wt% ethanol. Also, our results say nothing about the chain movement. At least the solvent is slower when ethanol is added. The increased counterion condensation also indicates the solvent to be poorer in the systems with added ethanol.

6.5 Water orientation around the polyelectrolyte

The previous chapters have already demonstrated that ethanol and urea have an effect on the interactions of PSS and PDADMA. One of the factors affecting the interaction of macromolecules is the hydration layer of the macromolecule. The number density maps and radial distribution functions demonstrated the existence of hydration layers around the PEs, both in single-PE systems and in the complex systems. To further understand the effects of the additives on the hydration layers of the PEs, the orientation of water dipoles around both of the PEs were studied for all single-PE and complex systems. Water dipole orientations for all single-PE and 2-PE systems are presented in Fig. 28 and Fig. 29.

The water dipole orientation is different around PSS and PDADMA due to their opposite charges. More peaks are seen in the water orientation around PSS than around PDADMA, which means that the water is more structured around PSS than around PDADMA. This results from the more localized charge of PSS in comparison to PDADMA. The results show that adding the second PE changes the water orientation significantly, especially around PDADMA. For PSS, the single-PE systems give slightly different results than the complex systems, but the trends are mostly similar. Addition of ethanol or urea seems to result in stronger water orientation around PSS in all systems. For PDADMA the results are opposite for single-PE systems and 2-PE systems. In PDADMA-only systems the orientation of the water dipole is stronger with increasing water content, whereas ethanol and urea make the orientation stronger in 2-PE systems. The absence of counterions of PDADMA in the 2-PE systems is most likely the reason for the notable difference in the water dipole orientation around PDADMA in 2-PE systems in comparison to the PDADMA-only systems. The charge distribution around the PDADMA chain is presumably quite different in the two cases, whereas for PSS, some counterions are present in all systems, and the changes between the systems are smaller than for PDADMA.

To verify if solvation shells form around the counterions, radial distribution functions were calculated between the ions and solvent molecules in single-PE systems (Fig. 30, 31, 32 and 33). All RDFs show at least one well-distinguishable peak. This indicates that there is at least one solvation shell around the ions. However, the counterions might be in the vicinity of the PE, and peaks might include the solvation shells of the polyelectrolyte. Solvent shell structure forms around the ions in all systems. This affects the solvent-PE interactions, as the solvent is differently structured in the vicinity of the counterions.

The results demonstrate that the water dipoles orientate strongly around the PEs, and this effect seems to extend to at least 1 nm from the PE complex. this is in line with atomistic simulations with classical MD performed by Qiao et al.[101]. These simulations of PSS/PDADMA bilayer in water show strong polarization of water, which is also observed here. The observable water polarization extends to a distance of a few nanometres from the surface of the layer[101], which is larger value than that obtained here. Nevertheless, the complex studied here is smaller than the bilayer structure studied by Qiao et al., which probably is the reason for the difference in

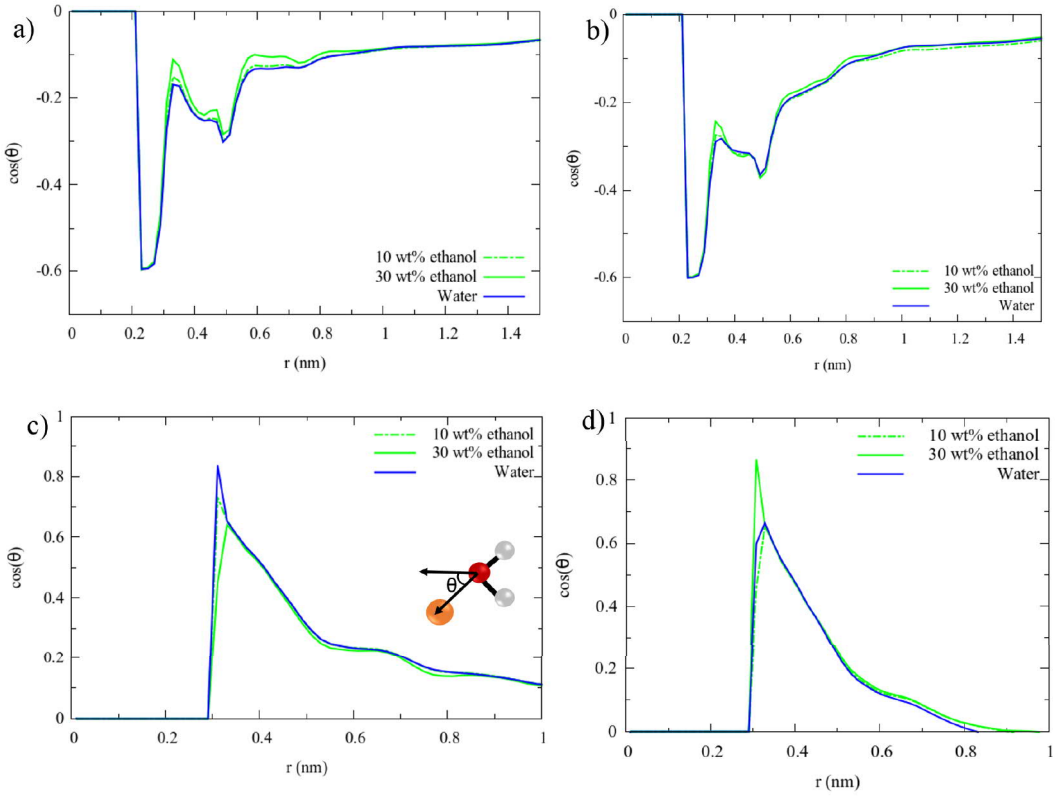

Figure 28: Water dipole orientation around a) PSS in single-PE system, b) PSS in 2-PE system, c) PDADMA in single-PE system and d) PDADMA in 2-PE system. θ is the angle between the water dipole and the polyelectrolyte charge group, see inset. Water orientation is very different around PSS and PDADMA. The addition of the second polyelectrolyte affects the water orientation greatly.

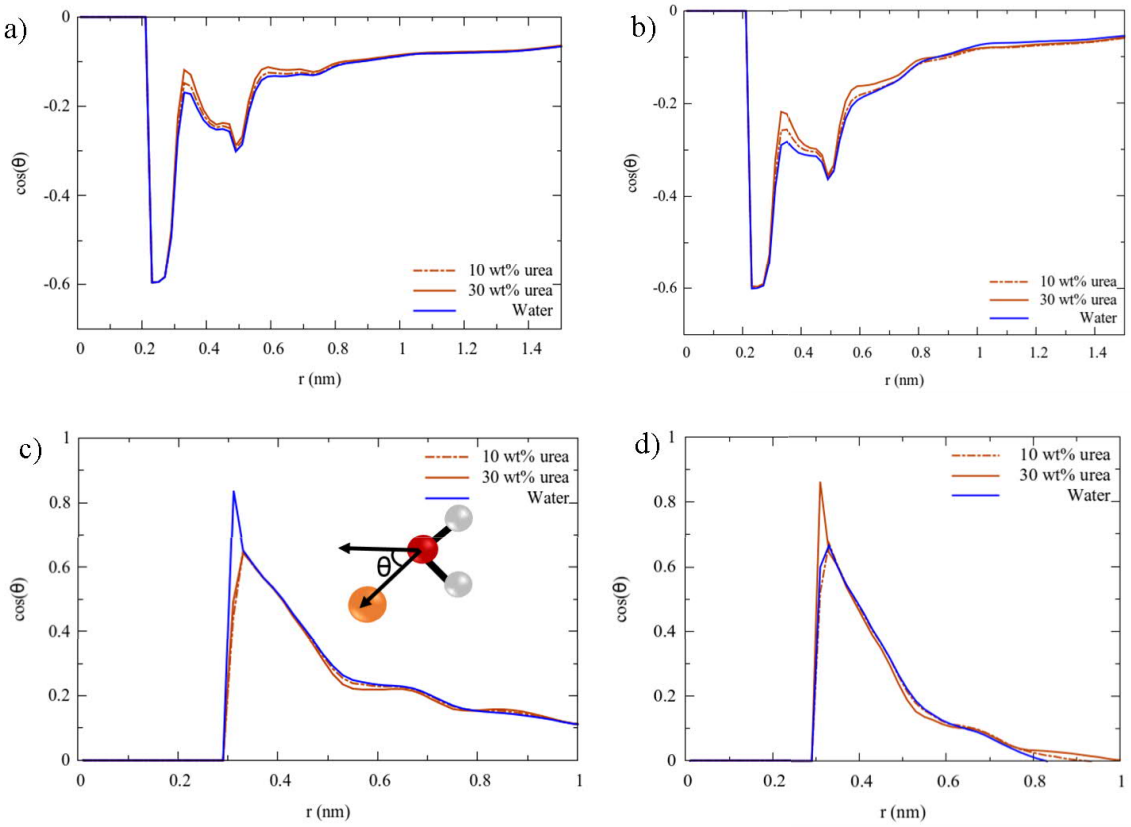

Figure 29: Water orientation around a) PSS in single-PE system, b) PSS in 2-PE system, c) PDADMA in single-PE system and PDADMA in 2-PE system. θ is the angle between the water dipole and the polyelectrolyte charge group.

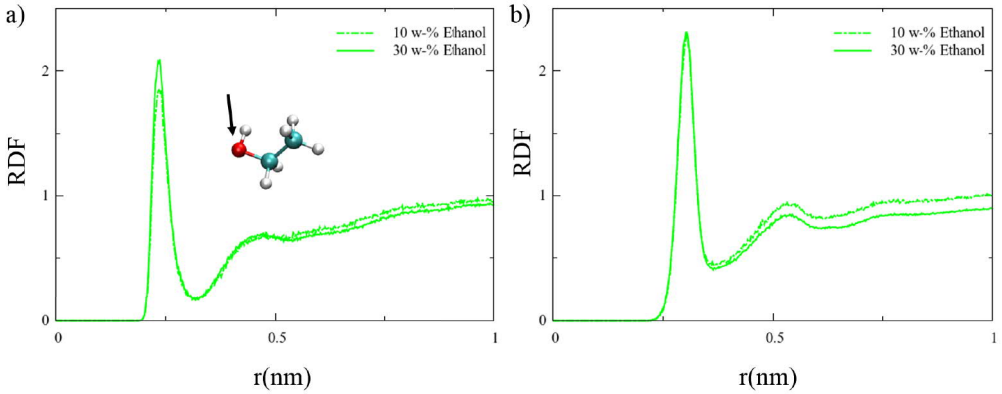

Figure 30: Radial distribution functions between a) chloride ions and ethanol hydroxyl group in PDADMA-only-systems and b) sodium ions and ethanol hydroxyl group in PSS-only-systems.

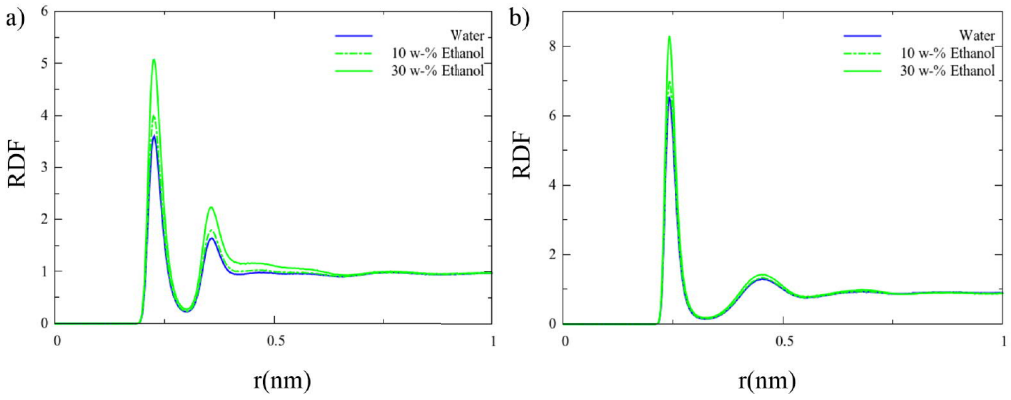

Figure 31: Radial distribution functions between a) chloride ions and water hydrogen atoms in PDADMA-only-systems and b) sodium ions and water oxygen atom in PSS-only-systems.

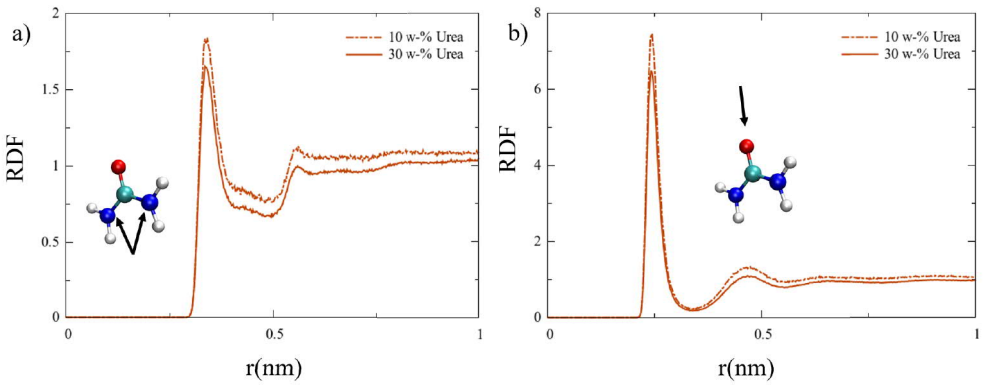

Figure 32: Radial distribution functions between a) chloride ions and urea nitrogen atoms in PDADMA-only-systems and b) sodium ions and urea oxygen atom in PSS-only-systems.

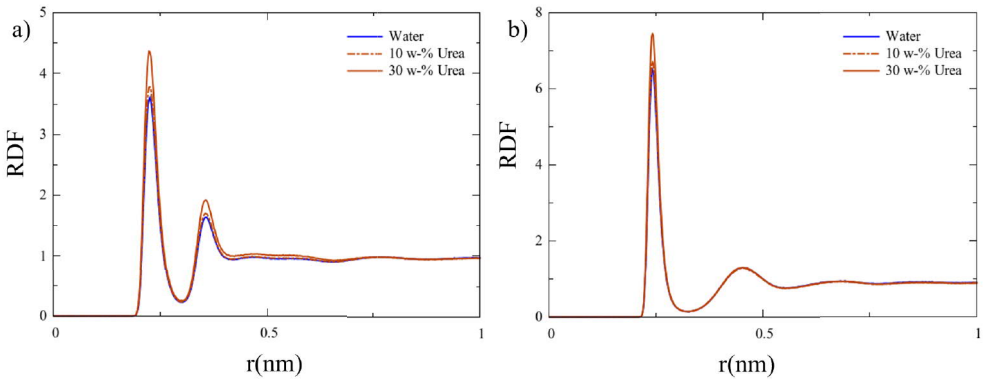

Figure 33: Radial distribution functions between a) chloride ions and water hydrogen atoms in PDADMA-only-systems and b) sodium ions and water oxygen atom in PSS-only-systems.

the solvent volume affected by the PE.

To conclude, urea and ethanol do change the water dipole orientation. In addition to the additives, the orientation of the water dipoles around PSS and PDADMA is affected by counterions, and the complexation with another PE. The water dipoles orientate more strongly around PSS with increasing ethanol and urea concentrations. The stronger water dipole orientation observed around PSS in all systems in the presence of additives could result from the change in the dielectric constant and hydrogen bonding network. The orientation does not tell whether the mechanism of the stronger orientation in the presence of urea is the same as in the ethanol systems.

To summarize all of the solvent behaviour analysis results described so far, ethanol and urea change the hydration shell structure of PSS and PDADMA by breaking PSS-water hydrogen bonds, slowing the diffusion of solvent, and changing the orientation and position of water molecules. These changes in the solvent affect the PSS-PDADMA interactions. Penetration of urea into the complex pushes the PEs apart, whereas ethanol keeps them close together. These results indicate that both ethanol and urea will affect the physical and mechanical properties of macroscopic PE materials. Increased polycation-polyanion distance caused by urea suggests a softening of PSS-PDADMA assemblies when urea is added. However, the decreased solvent diffusion rate suggests increased stiffness, as the diffusive water does not soften the assemblies as much as in pure water, where the water is more mobile. Urea and ethanol could also stabilise PSS-PDADMA complex materials, as it decreases the diffusion rate of the solvent. In addition to the possible changes in the mechanical properties and stability of macroscopic PE assemblies, effects on thermal properties are possible as well. For example, the temperature for the glass-transition like thermal transition discussed in Chapter 3 could increase, as the mobility of the chains is decreased by urea.

6.6 Ion condensation

When the small counterions remain in the vicinity of the polyelectrolyte, and cannot move freely in the solution, they are considered condensed. Counterion condensation is one of the principle phenomena in PE solutions. Its magnitude affects the effective charge of the PEs, and therefore the properties of PE assemblies. Finite concentrations of salt plasticize PE assemblies, and at high ionic strengths PE assemblies might completely fall apart, as intrinsic pairing (pairing between the monomers of the polycation and polyanion) decreases and extrinsic pairing (PE monomer charges pair with counterions) occurs more often[6,7]. The magnitude of the counterion condensation is dependent on the quality of the solvent: decreased dielectric constant and electrostatic screening result in higher counterion condensation.

Although in this thesis the number of small ions was very low in the 2-PE systems as the focus was on the solvent effects instead of salt effects, counterion condensation was studied due to its importance to the properties of PE complexes and assemblies. The numbers of ions were 10 Cl-ions in PDADMA-only systems, 20 Na-ions in PSS-only systems, and in the PSS-PDADMA systems 10 Na-ions to account for the 10 PSS charges not balanced by the charge of the PDADMA chain. The counterion

condensation was studied for all two-PE-systems. The condensation of sodium ions at PSS was estimated from cumulative radial distribution function calculated for PSS charge groups and the sodium ions (Fig. 34).

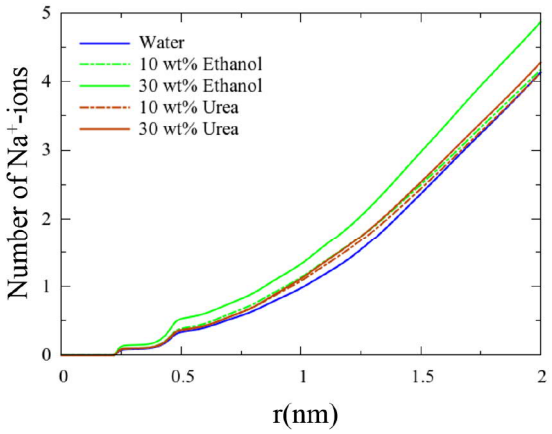

Figure 34: Cumulative 3D-radial distribution function between PSS sulfonate groups and sodium ions calculated for PSS-PDADMA systems shows highest counterion condensation in 30 wt% ethanol.

Highest counterion condensation occurs in the 30 wt% ethanol system, lowest in pure water. 10 wt% ethanol and both 10 wt% and 30 wt% systems show very similar counterion condensation magnitudes, all of them being slightly above that of water, and those of the urea systems being higher than the 10 wt% ethanol system. According to the obtained data, increasing ethanol concentration increases the counterion condensation. This effect could be a consequence of the decreased electrostatic screening of the solvent caused by the addition of ethanol, which in turn causes the charged and more polar species to go together in solution.

The results on the PSS-PDADMA backbone distance do not indicate that addition of ethanol would change the separation of PSS and PDADMA. However, the decrease in electrostatic screening would suggest that the chains would be closer together in the presence of ethanol, compared to pure water. On the other hand, this also means an increase in the counterion condensation, which in turn could decrease the intrinsic pairing of PSS and PDADMA, and possibly increase their separation. Also, the slow solvent diffusion rate in the 30 wt% ethanol indicates that the complex would be more stable. As the systems studied include only a very small number of counterions, the balance of these effects is not known.

To summarize the counterion condensation effects, all 2-PE-systems with additives showed stronger condensation than the pure water system, with especially high condensation in the 30 wt% ethanol system. As salt effects are of interest in PE materials engineering, e.g. for the plasticizing effects of salt, these results rise interest for the combined effect of finite salt amounts and ethanol. With the methods employed in this thesis, the study with larger number of ions would not significantly increase the computational cost, and would not complicate the modelling.

7 Conclusions

The effect of addition of ethanol and urea on the interactions of PSS and PDADMA was studied via classical molecular dynamics. The aim of the study was to assess the effect of solvent on the interactions of oppositely charged polyelectrolytes at molecular level. The results demonstrate that both ethanol and urea have an effect on the PSS-PDADMA backbone distance, ion condensation and solvent dynamics in the solution. These effects arise from the changes in the hydrogen bonding network and dielectric properties of the solvent caused by the addition of ethanol and urea.

Changes in the PE hydration layer structure were observed. Both ethanol and urea penetrate the formed PSS-PDADMA complex, urea being more abundant between the chains than ethanol. Both urea and ethanol affect the system entropy by interfering the water hydrogen bonding network. This was seen as changes in the water dipole orientation around the PEs. The dynamics of the solvent are also greatly altered by both additives. The diffusion coefficient of water in 2-PE systems is decreased by 21% from pure water system to the 30 wt% urea system and 47% from water to the 30 wt% ethanol system. The lifetime of hydrogen bonds between PSS and water is increased by both additives, while ethanol has greater effect than urea. The solvent additives have also enthalpic effects as they affect the magnitude of electrostatic interactions. This effect was especially pronounced for ethanol due to its low dielectric constant: it increases counterion condensation significantly due to decreased electrostatic screening. An increase in the ion condensation was observed for urea as well, but it was significantly smaller than for ethanol.

The results are interesting, because they indicate that both ethanol and urea could induce changes in the behaviour of larger PE assemblies. Urea and ethanol could be added either in the PEC formation/PEM deposition solution, or post-assembly. Urea could soften self-assembled PE materials, as it increases the PE backbone distances. Both ethanol and urea could affect thermal behaviour of PE assemblies due to their effect on the diffusion of the solvent. Ethanol could make PE assemblies stiffer, due to its dehydrating behaviour. Urea and ethanol demonstrate potential in controlling of properties of PEMs and PECs, such as stiffness and stability. These effects could possibly be employed in the processing and application of macroscopic polyelectrolyte materials. Changes in stiffness as a function of concentration of ethanol or urea could be employed for instance in sensors. Applications requiring higher temperatures could benefit from the increased stability of the complex possibly provided by both of these additives.

Although the results do reveal effects of ethanol and urea on PSS-PDADMA interactions, the thesis would have benefited from additional analysis, as for instance the energetics of the complexation were not studied. The binding strength would be an interesting thing to study, as the focus is on the interactions of PSS and PADMA, and the obtained results indicate that ethanol and urea could affect the binding strength. Also, the charge localization in the PE chains greatly influences the interactions between solvent and the macromolecule. Although PSS-PDADMA systems have been studied very widely and considered as a model system for strong PE complexes, and the results could point to the right direction also for other PE

systems, other systems should be studied in order to verify the effects on other PEs.

The thesis succeeded in revealing new information of the effect of solvent on the interactions of PSS and PDADMA. The thesis provides new insights to the effect of solvent on polycation-polyanion interactions in general. Overall, previous studies on the effect of solvent on polyelectrolyte complexes have been either experimental, or computational on larger systems, such as PE bilayers or PEMs[5,70]. Also, although PE solutions have been a focus of research for decades, to my knowledge, the effect of urea on polyanion-polycation interactions of strong polyelectrolytes has not been studied before. Therefore, this thesis provides a new perspective on the solvent effects in PEC-containing solutions.

The chosen methodology is a widely employed one with good comparability to both other computational results as well as experimental data. It allows the study of relatively small systems with chemical specificity. However, the computational costs rise due to the explicit atomic description, which limits the system size, which in turn introduces finite size effects. Due to sampling problem of finite-length simulations, the initial configurations influence the obtained results. In this thesis, the two datasets revealed this sampling problem to be quite significant. Additional datasets and longer simulation times would help to tackle this problem.

Although synthetic polyelectrolytes have been modelled with atomistic MD, force fields have not been parametrized for synthetic PEs, and as of now, comparisons on the suitability of different force fields on PE modelling have not been published. Thus, it would be beneficial to assess the suitability and strengths of widely employed force fields for these molecules, as they are remaining as a focus of research. In addition to classical force fields, polarizable force fields could reveal additional information for instance of the behaviour of water in the system, and they are already utilized to study systems of this size.

Applicability of the results is limited by the simple systems and methods used, therefore more research is required to verify the results and to extend to other systems. To further study the solvent quality for PEs, it would be beneficial to extend the study to freely moving PE chains. As the length of the chains utilized here is longer than their persistence length, the use of stretched, periodic chain prevents observing the chain conformation changes and estimating the solvent quality utilizing radius of gyration as a measure. Role of other additives, such as glycol, apolar organic solvents, or higher concentrations of ethanol and urea could provide more specific information on the role and characteristics of solvent-PE interactions. As both salt and solvent effect the distance and mobility of PE chains, the combined role of salt and additive would also be of interest, especially for ethanol systems.

This thesis broadens the understanding of solvent-PE interactions and adds to the not-so-wide field of atomistic simulations on PE complexes. Self-assembling PE materials are of interest for both industry and academia due to their tunable and functional properties, such as superhydrophobicity and supertensility. They are easy and cheap to produce, as they form spontaneously from water solutions. Thorough understanding of the phenomena related to these materials would allow efficient materials and applications developement. The results obtained in this study have interesting implications, but the connection to experimental work as well as

the applicability and transferability of the results is limited by the small system size, small number of datasets and the use of only PSS and PDADMA. Additional research is thus needed to verify the effects indicated by the results of this thesis, and to extend the research to other systems.

References

[1] M. A. Cohen Stuart, W. T. S. Huck, J. Genzer, M. Mueller, C. Ober, M. Stamm, G. B. Sukhorukov, I. Szleifer, V. V. Tsukruk, M. Urban, F. Winnik, S. Zauscher, I. Luzinov, and S. Minko, "Emerging applications of stimuli-responsive polymer materials," *Nature Materials*, vol. 9, no. 2, pp. 101–113, 2010.

[2] M. Muthukumar, "50th anniversary perspective: A perspective on polyelectrolyte solutions," *Macromolecules*, vol. 50, no. 24, pp. 9528–9560, 2017.

[3] G. Decher, "Fuzzy nanoassemblies: Toward layered polymeric multicomposites," *Science*, vol. 277, no. 5330, pp. 1232–1237, 1997.

[4] S. S. Shiratori and M. F. Rubner, "ph-dependent thickness behavior of sequentially adsorbed layers of weak polyelectrolytes," *Macromolecules*, vol. 33, no. 11, pp. 4213–4219, 2000.

[5] S. T. Dubas and J. B. Schlenoff, "Factors controlling the growth of polyelectrolyte multilayers," *Macromolecules*, vol. 32, no. 24, pp. 8153–8160, 1999.

[6] Q. Wang and J. B. Schlenoff, "The polyelectrolyte complex/coacervate continuum," *Macromolecules*, vol. 47, no. 9, pp. 3108–3116, 2014.

[7] J. A. Jaber and J. B. Schlenoff, "Counterions and water in polyelectrolyte multilayers: A tale of two polycations," *Langmuir*, vol. 23, no. 2, pp. 896–901, 2007.

[8] E. Guzman, H. Ritacco, J. E. F. Rubio, R. G. Rubio, and F. Ortega, "Salt-induced changes in the growth of polyelectrolyte layers of poly(diallyldimethylammonium chloride) and poly(4-styrene sulfonate of sodium)," *Soft Matter*, vol. 50, pp. 2130–2142, 20090.

[9] J. Hiller, J. Mendelsohn, and M. Rubner, "Reversibly erasable nanoporous anti-reflection coatings from polyelectrolyte multilayers," *Nature Materials*, vol. 1, no. 1, pp. 59–63, 2002.

[10] D. S. Hwang, J. H. Waite, and M. Tirrell, "Promotion of osteoblast proliferation on complex coacervation-based hyaluronic acid - recombinant mussel adhesive protein coatings on titanium," *Biomaterials*, vol. 31, no. 6, pp. 1080–1084, 2010.

[11] D. S. Hwang, H. Zeng, A. Srivastava, D. V. Krogstad, M. Tirrell, J. N. Israelachvili, and J. H. Waite, "Viscosity and interfacial properties in a mussel-inspired adhesive coacervate," *Soft Matter*, vol. 6, no. 14, pp. 3232–3236, 2010.

[12] P. Yusan, I. Tuncel, V. Butun, A. L. Demirel, and I. Erel-Goktepe, "pH-responsive layer-by-layer films of zwitterionic block copolymer micelles," *Polymer Chemistry*, vol. 5, no. 12, pp. 3777–3787, 2014.

[13] E. Yildirim, Y. Zhang, J. L. Lutkenhaus, and M. Sammalkorpi, "Thermal transitions in polyelectrolyte assemblies occur via a dehydration mechanism," *ACS Macro Letters*, vol. 4, no. 9, pp. 1017–1021, 2015.

[14] E. Poptoshev, B. Schoeler, and F. Caruso, "Influence of solvent quality on the growth of polyelectrolyte multilayers," *Langmuir*, vol. 20, no. 3, pp. 829–834, 2004.

[15] A. S. Michaels, "Polyelectrolyte complexes," *Industrial & Engineering Chemistry*, vol. 57, no. 10, pp. 32–40, 1965.

[16] Y. Gu, Y. Ma, B. D. Vogt, and N. S. Zacharia, "Contraction of weak polyelectrolyte multilayers in response to organic solvents," *Soft Matter*, vol. 12, no. 6, pp. 1859–1867, 2016.

[17] A. Ghoufi, F. Artzner, and P. Malfreyt, "Physical properties and hydrogen-bonding network of water–ethanol mixtures from molecular dynamics simulations," *The Journal of Physical Chemistry B*, vol. 120, no. 4, pp. 793–802, 2016.

[18] A. Masunov and J. J. Dannenberg, "Theoretical study of urea and thiourea. 2. chains and ribbons," *The Journal of Physical Chemistry B*, vol. 104, no. 4, pp. 806–810, 2000.

[19] A. V. Dobrynin and M. Rubinstein, "Theory of polyelectrolytes in solutions and at surfaces," *Progress in Polymer Science*, vol. 30, no. 11, pp. 1049 – 1118, 2005.

[20] G. S. Manning, "Limiting laws and counterion condensation in polyelectrolyte solutions i. colligative properties," *The Journal of Chemical Physics*, vol. 51, no. 3, pp. 924–933, 1969.

[21] C. Patra and L. Bhuiyan, "The effect of ionic size on polyion-small ion distributions in a cylindrical double layer," *Condensed Matter Physics*, vol. 8, no. 2, pp. 425–446, 2005.

[22] L. B. Bhuiyan and C. W. Outhwaite, "Comparison of exclusion volume corrections to the Poisson-Boltzmann equation for inhomogeneous electrolytes," *Journsal of Colloid and Interface Science*, vol. 331, no. 2, pp. 543–547, 2009.

[23] R. De, H. Lee, and B. Das, "Exploring the interactions in binary mixtures of polyelectrolytes: Influence of mixture composition, concentration, and temperature on counterion condensation," *Journal of Molecular Liquids*, vol. 251, pp. 94 – 99, 2018.

[24] D. Volodkin and R. von Klitzing, "Competing mechanisms in polyelectrolyte multilayer formation and swelling: Polycation–polyanion pairing vs. polyelectrolyte–ion pairing," *Current Opinion in Colloid and Interface Science*, vol. 19, no. 1, pp. 25 – 31, 2014.

[25] F. Oosawa, *Polyelectrolytes*. New York, USA: Marcel Dekker, 1 ed., 1971.

[26] M. Deserno, C. Holm, and S. May, "Fraction of condensed counterions around a charged rod: Comparison of Poisson-Boltzmann theory and computer simulations," *Macromolecules*, vol. 33, no. 1, pp. 199–206, 2000.

[27] V. Perel and B. Shklovskii, "Screening of a macroion by multivalent ions: a new boundary condition for the Poisson-Boltzmann equation and charge inversion," *Physica A*, vol. 274, no. 3-4, pp. 446–453, 1999.

[28] B. Ha and A. Liu, "Effect of non-pairwise-additive interactions on bundles of rodlike polyelectrolytes," *Physical Review Letters*, vol. 81, no. 5, pp. 1011–1014, 1998.

[29] P. Batys, S. Luukkonen, and M. Sammalkorpi, "Ability of the Poisson-Boltzmann equation to capture molecular dynamics predicted ion distribution around polyelectrolytes," *Physical Chemistry Chemical Physics*, vol. 19, no. 36, pp. 24583–24593, 2017.

[30] M. Deserno, F. Jiménez-Ángeles, C. Holm, and M. Lozada-Cassou, "Overcharging of DNA in the presence of salt: Theory and simulation," *The Journal of Physical Chemistry B*, vol. 105, no. 44, pp. 10983–10991, 2001.

[31] E. Trizac and G. Téllez, "Onsager-manning-oosawa condensation phenomenon and the effect of salt," vol. 96, p. 038302, 2006.

[32] B. Ha and A. Liu, "Counterion-mediated attraction between two like-charged rods," *Physical Review Letters*, vol. 79, no. 7, pp. 1289–1292, 1997.

[33] A. Kundagrami and M. Muthukumar, "Theory of competitive counterion adsorption on flexible polyelectrolytes: Divalent salts," *Journal of Chemical Physics*, vol. 128, no. 24, 2008.

[34] Y. D. Gordievskaya, A. A. Gavrilov, and E. Y. Kramarenko, "Effect of counterion excluded volume on the conformational behavior of polyelectrolyte chains," *Soft Matter*, vol. 14, pp. 1474–1481, 2018.

[35] M. Rubinstein and R. H. Colby, *Polymer Physics*. Oxford University Press, 2003.

[36] P. J. Flory, "Spatial configuration of macromolecular chains," *Science*, vol. 188, no. 4195, pp. 1268–1276, 1975.

[37] A. Yethiraj, "Liquid state theory of polyelectrolyte solutions," *The Journal of Physical Chemistry B*, vol. 113, no. 6, pp. 1539–1551, 2009.

[38] A. V. Dobrynin, M. Rubinstein, and S. P. Obukhov, "Cascade of transitions of polyelectrolytes in poor solvents," *Macromolecules*, vol. 29, no. 8, pp. 2974–2979, 1996.

[39] R. Fuoss, "Viscosity Function for Polyelectrolytes," *Journal of Polymer Science*, vol. 3, no. 4, pp. 603–604, 1948.

[40] N. T. M. Klooster, F. Van der Touw, and M. Mandel, "Solvent effects in polyelectrolyte solutions. 1. potentiometric and viscosimetric titration of poly(acrylic acid) in methanol and counterion specificity," *Macromolecules*, vol. 17, no. 10, pp. 2070–2078, 1984.

[41] J. B. Schlenoff, H. Ly, and M. Li, "Charge and mass balance in polyelectrolyte multilayers," *Journal of the American Chemical Society*, vol. 120, no. 30, pp. 7626–7634, 1998.

[42] H. Riegler and F. Essler, "Polyelectrolytes. 2. intrinsic or extrinsic charge compensation? quantitative charge analysis of PAH/PSS multilayers," *Langmuir*, vol. 18, no. 17, pp. 6694–6698, 2002.

[43] N. Kotov, "Layer-by-layer self-assembly: the contribution of hydrophobic interactions," *Nanostructured Materials*, vol. 12, no. 5-8, pp. 789–796, 1999.

[44] J. Fu and J. B. Schlenoff, "Driving forces for oppositely charged polyion association in aqueous solutions: Enthalpic, entropic, but not electrostatic," *Journal of the American Chemical Society*, vol. 138, no. 3, pp. 980–990, 2016.

[45] M. Castelnovo and J.-F. Joanny, "Complexation between oppositely charged polyelectrolytes: Beyond the random phase approximation," *The European Physical Journal E*, vol. 6, no. 1, pp. 377–386, 2001.

[46] P. M. Biesheuvel and M. A. Cohen Stuart, "Electrostatic free energy of weakly charged macromolecules in solution and intermacromolecular complexes consisting of oppositely charged polymers," *Langmuir*, vol. 20, no. 7, pp. 2785–2791, 2004.

[47] R. de Vries and M. Cohen Stuart, "Theory and simulations of macroion complexation," *Current Opinion in Colloid and Interface Science*, vol. 11, no. 5, pp. 295 – 301, 2006.

[48] T. P. Silverstein, "The real reason why oil and water don't mix," *Journal of Chemical Education*, vol. 75, no. 1, p. 116, 1998.

[49] Z. Ou and M. Muthukumar, "Entropy and enthalpy of polyelectrolyte complexation: Langevin dynamics simulations," *The Journal of Chemical Physics*, vol. 124, no. 15, p. 154902, 2006.

[50] K. Kaibara, T. Okazaki, H. B. Bohidar, and P. L. Dubin, "pH-induced coacervation in complexes of bovine serum albumin and cationic polyelectrolytes," *Biomacromolecules*, vol. 1, no. 1, pp. 100–107, 2000.

[51] B. P. Das and M. Tsianou, "From polyelectrolyte complexes to polyelectrolyte multilayers: Electrostatic assembly, nanostructure, dynamics, and functional properties," *Advances in Colloid and Interface Science*, vol. 244, pp. 71 – 89, 2017. Special Issue in Honor of the 90th Birthday of Prof. Eli Ruckenstein.

[52] J. Fu, H. M. Fares, and J. B. Schlenoff, "Ion-pairing strength in polyelectrolyte complexes," *Macromolecules*, vol. 50, no. 3, pp. 1066–1074, 2017.

[53] V. S. Meka, M. K. Sing, M. R. Pichika, S. R. Nali, V. R. Kolapalli, and P. Kesharwani, "A comprehensive review on polyelectrolyte complexes," *Drug Discovery Today*, vol. 22, no. 11, pp. 1697 – 1706, 2017.

[54] A. J. Nolte, N. D. Treat, R. E. Cohen, and M. F. Rubner, "Effect of relative humidity on the Young's modulus of polyelectrolyte multilayer films and related nonionic polymers," *Macromolecules*, vol. 41, no. 15, pp. 5793–5798, 2008.

[55] C. E. Sing, "Development of the modern theory of polymeric complex coacervation," *Advances in Colloid and Interface Science*, vol. 239, pp. 2 – 16, 2017.

[56] M. Salomäki, I. A. Vinokurov, and J. Kankare, "Effect of temperature on the buildup of polyelectrolyte multilayers," *Langmuir*, vol. 21, no. 24, pp. 11232–11240, 2005.

[57] K. Sadman, Q. Wang, Y. Chen, B. Keshavarz, Z. Jiang, and K. R. Shull, "Influence of hydrophobicity on polyelectrolyte complexation," *Macromolecules*, vol. 50, no. 23, pp. 9417–9426, 2017.

[58] K. Köhler, D. G. Shchukin, H. Möhwald, and G. B. Sukhorukov, "Thermal behavior of polyelectrolyte multilayer microcapsules. 1. the effect of odd and even layer number," *The Journal of Physical Chemistry B*, vol. 109, no. 39, pp. 18250–18259, 2005.

[59] J. T. O'Neal, E. Y. Dai, Y. Zhang, K. B. Clark, K. G. Wilcox, I. M. George, N. E. Ramasamy, D. Enriquez, P. Batys, M. Sammalkorpi, and J. L. Lutkenhaus, "QCM-D investigation of swelling behavior of layer-by-layer thin films upon exposure to monovalent ions," *Langmuir*, vol. 34, no. 3, pp. 999–1009, 2018.

[60] R. Zhang, Y. Zhang, H. S. Antila, J. L. Lutkenhaus, and M. Sammalkorpi, "Role of salt and water in the plasticization of PDAC/PSS polyelectrolyte assemblies," *The Journal of Physical Chemistry B*, vol. 121, no. 1, pp. 322–333, 2017.

[61] K. Köhler, H. Möhwald, and G. B. Sukhorukov, "Thermal behavior of polyelectrolyte multilayer microcapsules: 2. insight into molecular mechanisms for the PDADMAC/PSS system," *The Journal of Physical Chemistry B*, vol. 110, no. 47, pp. 24002–24010, 2006.

[62] O. Soltwedel, P. Nestler, H.-G. Neumann, M. Paßvogel, R. Köhler, and C. A. Helm, "Influence of polycation (PDADMAC) weight on vertical diffusion within polyelectrolyte multilayers during film formation and postpreparation treatment," *Macromolecules*, vol. 45, no. 19, pp. 7995–8004, 2012.

[63] A. V. Kabanov, T. K. Bronich, V. A. Kabanov, K. Yu, and A. Eisenberg, "Soluble stoichiometric complexes from poly(n-ethyl-4-vinylpyridinium) cations and poly(ethylene oxide)-block-polymethacrylate anions," *Macromolecules*, vol. 29, no. 21, pp. 6797–6802, 1996.

[64] J.-F. Gohy, S. K. Varshney, and R. Jérôme, "Water-soluble complexes formed by poly(2-vinylpyridinium)-block-poly(ethylene oxide) and poly(sodium methacrylate)-block-poly(ethylene oxide) copolymers," *Macromolecules*, vol. 34, no. 10, pp. 3361–3366, 2001.

[65] N. Laugel, C. Betscha, M. Winterhalter, J.-C. Voegel, P. Schaaf, and V. Ball, "Relationship between the growth regime of polyelectrolyte multilayers and the polyanion/polycation complexation enthalpy," *The Journal of Physical Chemistry B*, vol. 110, no. 39, pp. 19443–19449, 2006.

[66] B. Hofs, I. K. Voets, A. de Keizer, and M. A. Cohen Stuart, "Comparison of complex coacervate core micelles from two diblock copolymers or a single diblock copolymer with a polyelectrolyte," *Physical Chemistry Chemical Physics*, vol. 8, no. 36, pp. 4242–4251, 2006.

[67] J. H. Ortony, B. Qiao, C. J. Newcomb, T. J. Keller, L. C. Palmer, E. Deiss-Yehiely, M. Olvera de la Cruz, S. Han, and S. I. Stupp, "Water dynamics from the surface to the interior of a supramolecular nanostructure," *Journal of the American Chemical Society*, vol. 139, no. 26, pp. 8915–8921, 2017.

[68] B. Bagchi, "Water dynamics in the hydration layer around proteins and micelles," *Chemical Reviews*, vol. 105, no. 9, pp. 3197–3219, 2005.

[69] J. Borges and J. F. Mano, "Molecular Interactions Driving the Layer-by-Layer Assembly of Multilayers," *Chemical Reviews*, vol. 114, no. 18, pp. 8883–8942, 2014.

[70] M. D. Miller and M. L. Bruening, "Correlation of the swelling and permeability of polyelectrolyte multilayer films," *Chemistry of Materials*, vol. 17, no. 21, pp. 5375–5381, 2005.

[71] E. Kokufuta, H. Suzuki, R. Yoshida, K. Yamada, M. Hirata, and F. Kaneko, "Role of hydrogen bonding and hydrophobic interaction in the volume collapse of a poly(ethylenimine) gel," *Langmuir*, vol. 14, no. 4, pp. 788–795, 1998.

[72] E. Kokufuta, B. Wang, R. Yoshida, A. R. Khokhlov, and M. Hirata, "Volume phase transition of polyelectrolyte gels with different charge distributions," *Macromolecules*, vol. 31, no. 20, pp. 6878–6884, 1998.

[73] Y. Zhang, F. Li, L. D. Valenzuela, M. Sammalkorpi, and J. L. Lutkenhaus, "Effect of water on the thermal transition observed in poly(allylamine hydrochloride)–poly(acrylic acid) complexes," *Macromolecules*, vol. 49, no. 19, pp. 7563–7570, 2016.

[74] A. Vidyasagar, C. Sung, R. Gamble, and J. L. Lutkenhaus, "Thermal transitions in dry and hydrated layer-by-layer assemblies exhibiting linear and exponential growth," *ACS Nano*, vol. 6, no. 7, pp. 6174–6184, 2012.

[75] J. V. de Vondele, M. Krack, F. Mohamed, M. Parrinello, T. Chassaing, and J. Hutter, "Quickstep: Fast and accurate density functional calculations using a mixed gaussian and plane waves approach," *Computer Physics Communications*, vol. 167, no. 2, pp. 103 – 128, 2005.

[76] W. F. van Gunsteren, D. Bakowies, R. Baron, I. Chandrasekhar, M. Christen, X. Daura, P. Gee, D. P. Geerke, A. Glättli, P. H. Hünenberger, M. A. Kastenholz, C. Oostenbrink, M. Schenk, D. Trzesniak, N. F. A. van der Vegt, and H. B. Yu, "Biomolecular modeling: Goals, problems, perspectives," *Angewandte Chemie International Edition*, vol. 45, no. 25, pp. 4064–4092.

[77] A. R. Leach, *Molecular modelling: principles and applications*. United Kingdom: Pearson education, 2 ed., 2001.

[78] S. C. Glotzer and W. Paul, "Molecular and mesoscale simulation methods for polymer materials," *Annual Review of Materials Research*, vol. 32, no. 1, pp. 401–436, 2002.

[79] M. O. Steinhauser and S. Hiermaier, "A Review of Computational Methods in Materials Science: Examples from Shock-Wave and Polymer Physics," *International Journal of Molecular Sciences*, vol. 10, no. 12, pp. 5135–5216, 2009.

[80] S. C. Glotzer, "Computer simulations of spinodal decomposition in polymer blends," in *Annual Reviews of Computational Physics II*, pp. 1–46, World Scientific, 1995.

[81] L. Monticelli and E. Salonen, *Biomolecular Simulations: Methods and Protocols*. New York, USA: Humana Press, 1 ed., 2016.

[82] W. Damm, A. Frontera, J. Tirado–Rives, and W. L. Jorgensen, "OPLS all-atom force field for carbohydrates," *Journal of Computational Chemistry*, vol. 18, no. 16, pp. 1955–1970, 1997.

[83] W. L. Jorgensen, D. S. Maxwell, and J. Tirado-Rives, "Development and testing of the OPLS all-atom force field on conformational energetics and properties of organic liquids," *Journal of the American Chemical Society*, vol. 118, no. 45, pp. 11225–11236, 1996.

[84] A. D. Mackerell, "Empirical force fields for biological macromolecules: Overview and issues," *Journal of Computational Chemistry*, vol. 25, no. 13, pp. 1584–1604, 2004.

[85] G. Kaminski, E. M. Duffy, T. Matsui, and W. L. Jorgensen, "Free energies of hydration and pure liquid properties of hydrocarbons from the OPLS all-atom model," *The Journal of Physical Chemistry*, vol. 98, no. 49, pp. 13077–13082, 1994.

[86] B. Qiao, J. J. Cerdà, and C. Holm, "Poly(styrenesulfonate)-poly(diallyldimethylammonium) mixtures: Toward the understanding of polyelectrolyte complexes and multilayers via atomistic simulations," *Macromolecules*, vol. 43, no. 18, pp. 7828–7838, 2010.

[87] B. Qiao, M. Sega, and C. Holm, "An atomistic study of a poly(styrene sulfonate)/poly(diallyldimethylammonium) bilayer: the role of surface properties and charge reversal," *Physical Chemistry Chemical Physics*, vol. 13, no. 36, pp. 16336–16342, 2011.

[88] Y. Zhang, P. Batys, J. T. O'Neal, F. Li, M. Sammalkorpi, and J. L. Lutkenhaus, "Molecular origin of the glass transition in polyelectrolyte assemblies," *ACS Central Science*, vol. 4, no. 5, pp. 638–644, 2018.

[89] W. L. Jorgensen, J. Chandrasekhar, J. D. Madura, R. W. Impey, and M. L. Klein, "Comparison of simple potential functions for simulating liquid water," *The Journal of Chemical Physics*, vol. 79, no. 2, pp. 926–935, 1983.

[90] G. W. Slater, C. Holm, M. V. Chubynsky, H. W. de Haan, A. Dubé, K. Grass, O. A. Hickey, C. Kingsburry, D. Sean, T. N. Shendruk, and L. Zhan, "Modeling the separation of macromolecules: A review of current computer simulation methods," *Electrophoresis*, vol. 30, no. 5, pp. 792–818, 2009.

[91] R. Hockney, "Potential calculation and some applications," *Methods Comput. Phys. 9: 135-211.*, 1970.

[92] P. P. Ewald, "Die berechnung optischer und elektrostatischer gitterpotentiale," *Annalen der Physik*, vol. 369, no. 3, pp. 253–287, 1921.

[93] G. Bussi, D. Donadio, and M. Parrinello, "Canonical sampling through velocity rescaling," *The Journal of Chemical Physics*, vol. 126, no. 1, p. 014101, 2007.

[94] H. J. C. Berendsen, J. P. M. Postma, W. F. van Gunsteren, A. DiNola, and J. R. Haak, "Molecular dynamics with coupling to an external bath," *The Journal of Chemical Physics*, vol. 81, no. 8, pp. 3684–3690, 1984.

[95] M. Parrinello and A. Rahman, "Polymorphic transitions in single crystals: A new molecular dynamics method," *Journal of Applied Physics*, vol. 52, no. 12, pp. 7182–7190, 1981.

[96] M. G. Guenza, "Theoretical models for bridging timescales in polymer dynamics," *Journal of Physics-Condensed Matter*, vol. 20, no. 3, 2008.

[97] S. Glotzer and W. Paul, "Molecular and mesoscale simulation methods for polymer materials," *Annual Review of Materials Research*, vol. 32, pp. 401–436, 2002.

[98] M. Kosmas and K. Freed, "Scaling Theories of Polymer-Solutions," *Journal of Chemical physics*, vol. 69, no. 8, pp. 3647–3659, 1978.

[99] P. J. Flory, "Thermodynamics of high polymer solutions," *The Journal of Chemical Physics*, vol. 10, no. 1, pp. 51–61, 1942.

[100] Q. Zhang, J. Lin, L. Wang, and Z. Xu, "Theoretical modeling and simulations of self-assembly of copolymers in solution," *Progress in Polymer Science*, vol. 75, pp. 1–30, 2017.

[101] B.-F. Qiao, M. Sega, and C. Holm, "Properties of water in the interfacial region of a polyelectrolyte bilayer adsorbed onto a substrate studied by computer simulations," *Physical Chemistry Chemical Physics*, vol. 14, no. 32, pp. 11425–11432, 2012.

[102] M. Vögele, C. Holm, and J. Smiatek, "Coarse-grained simulations of polyelectrolyte complexes: MARTINI models for poly(styrene sulfonate) and poly(diallyldimethylammonium)," *The Journal of Chemical Physics*, vol. 143, no. 24, p. 243151, 2015.

[103] B. Hess, C. Kutzner, D. van der Spoel, and E. Lindahl, "GROMACS 4: Algorithms for highly efficient, load-balanced, and scalable molecular simulation," *Journal of Chemical Theory and Computation*, vol. 4, no. 3, pp. 435–447, 2008.

[104] W. L. Jorgensen and J. Tirado-Rives, "The OPLS [optimized potentials for liquid simulations] potential functions for proteins, energy minimizations for crystals of cyclic peptides and crambin," *Journal of the American Chemical Society*, vol. 110, no. 6, pp. 1657–1666, 1988.

[105] E. Duffy, S. D., and W. Jorgensen, "Urea - Potential Functions, log-P, and Free-Energy of Hydration," *Israel Journal of Chemistry*, vol. 33, no. 3, pp. 323–330, 1993.

[106] T. Darden, D. York, and L. Pedersen, "Particle mesh ewald: An N*log(N) method for ewald sums in large systems," *The Journal of Chemical Physics*, vol. 98, no. 12, pp. 10089–10092, 1993.

[107] B. Hess, H. Bekker, H. Berendsen, and J. Fraaije, "LINCS: A linear constraint solver for molecular simulations," *Journal of Computational Chemistry*, vol. 18, no. 12, pp. 1463–1472, 1997.

[108] M. P. Allen and D. J. Tildesley, *Computer simulation of liquids*. Oxford university press, 2017.

[109] A. Wakisaka and K. Matsuura, "Microheterogeneity of ethanol-water binary mixtures observed at the cluster level," *Journal of Molecular Liquids*, vol. 129, no. 1-2, pp. 25–32, 2006.

[110] C. Zhang and X. Yang, "Molecular dynamics simulation of ethanol/water mixtures for structure and diffusion properties," *Fluid Phase Equilibria*, vol. 231, no. 1, pp. 1–10, 2005.

[111] H. Kokubo and B. M. Pettitt, "Preferential solvation in urea solutions at different concentrations: properties from simulation studies," *The journal of physical chemistry B*, vol. 111, no. 19, pp. 5233–5242, 2007.

[112] G. S. Kell, "Density, thermal expansivity, and compressibility of liquid water from 0deg to 150deg. correlations and tables for atmospheric pressure and saturation reviewed and expressed on 1968 temperature scale," *Journal of Chemical & Engineering Data*, vol. 20, no. 1, pp. 97–105, 1975.

[113] I. S. Khattab, F. Bandarkar, M. A. A. Fakhree, and A. Jouyban, "Density, viscosity, and surface tension of water plus ethanol mixtures from 293 to 323 K," *Korean Journal of Chemicals Engineering*, vol. 29, no. 6, pp. 812–817, 2012.

[114] A. W. Hakin, C. L. Beswick, and M. M. Duke, "Thermochemical and volumetric properties of aqueous urea systems. heat capacities and volumes of transfer from water to urea-water mixtures for some 1 : 1 electrolytes at 298.15 K," *J. Chem. Soc., Faraday Trans.*, vol. 92, pp. 207–213, 1996.

[115] M. Lingenheil, R. Denschlag, R. Reichold, and P. Tavan, "The "hot-solvent/cold-solute" problem revisited," *Journal of Chemical Theory and Computation*, vol. 4, no. 8, pp. 1293–1306, 2008.

[116] J. Smiatek, A. Wohlfarth, and C. Holm, "The solvation and ion condensation properties for sulfonated polyelectrolytes in different solvents-a computational study," *New Journal of Physics*, vol. 16, 2014.

[117] M. Matsumoto, "Relevance of hydrogen bond definitions in liquid water," *Journal of Chemical Physics*, vol. 126, no. 5, 2007.